# **Efficient Transferable Optimal Transport via Min-Sliced Transport Plans**

Xinran Liu<sup>1</sup> Elaheh Akbari<sup>1</sup> Rocio Diaz Martin<sup>2</sup> Navid Naderi Alizadeh<sup>3</sup> Soheil Kolouri<sup>1,4</sup>

<sup>1</sup>Department of Computer Science, Vanderbilt University

<sup>2</sup>Department of Mathematics, Florida State University

<sup>3</sup>Department of Biostatistics & Bioinformatics, Duke University

<sup>4</sup>Department of Electrical & Computer Engineering, Vanderbilt University

### **Abstract**

Optimal Transport (OT) offers a powerful framework for finding correspondences between distributions and addressing matching and alignment problems in various areas of computer vision, including shape analysis, image generation, and multimodal tasks. The computation cost of OT, however, hinders its scalability. Slice-based transport plans have recently shown promise for reducing the computational cost by leveraging the closed-form solutions of 1D OT problems. These methods optimize a one-dimensional projection (slice) to obtain a conditional transport plan that minimizes the transport cost in the ambient space. While efficient, these methods leave open the question of whether learned optimal slicers can transfer to new distribution pairs under distributional shift. Understanding this transferability is crucial in settings with evolving data or repeated OT computations across closely related distributions. In this paper, we study the min-Sliced Transport Plan (min-STP) framework and investigate the transferability of optimized slicers: can a slicer trained on one distribution pair yield effective transport plans for new, unseen pairs? Theoretically, we show that optimized slicers remain close under slight perturbations of the data distributions, enabling efficient transfer across related tasks. To further improve scalability, we introduce a minibatch formulation of min-STP and provide statistical guarantees on its accuracy. Empirically, we demonstrate that the transferable min-STP achieves strong one-shot matching performance and facilitates amortized training for point cloud alignment and flow-based generative modeling. Our code is available at https://github.com/xinranliueva/Min-STP.

#### 1. Introduction

Many tasks in computer vision, natural language processing, biology, and operations research involve establishing correspondences between samples drawn from two distributions; a problem elegantly framed through the lens of optimal transport (OT) [34, 45]. OT provides a principled framework for determining the most efficient coupling between distributions while minimizing a transport cost, consistent with the principle of least effort (or least action) in transferring mass. Over the past decade, OT has been applied across a broad range of domains, including domain adaptation [11, 13], generative modeling [4, 16, 25], shape and image matching [5, 37, 41], word-embedding alignment [20, 49], single-cell analysis [39, 48], and resource allocation [17], among many others [21].

Despite its success, OT remains computationally expensive, with a complexity that scales cubically in the number of samples [34]. To address this bottleneck, a large body of research has sought scalable approximations, including entropic regularization [3, 12], low-rank and linearized formulations [38, 46], and hierarchical or multiscale methods [15, 18, 40]. Slicing-based techniques [6, 7, 23] form another efficient class of methods, reducing high-dimensional problems to a set of one-dimensional projections. While effective for computing OT distances, these methods do not recover explicit transportation plans. Recent extensions [9, 28, 29, 36] have begun to bridge this gap by constructing one-dimensional transportation plans along slices and lifting them to the ambient space to obtain transportation plans between input distributions.

However, all existing efficient OT methods are designed for single-instance problems. In many real-world applications, one must repeatedly solve OT between evolving or structurally similar distributions, where valuable information from prior solutions remains unused. Even when two

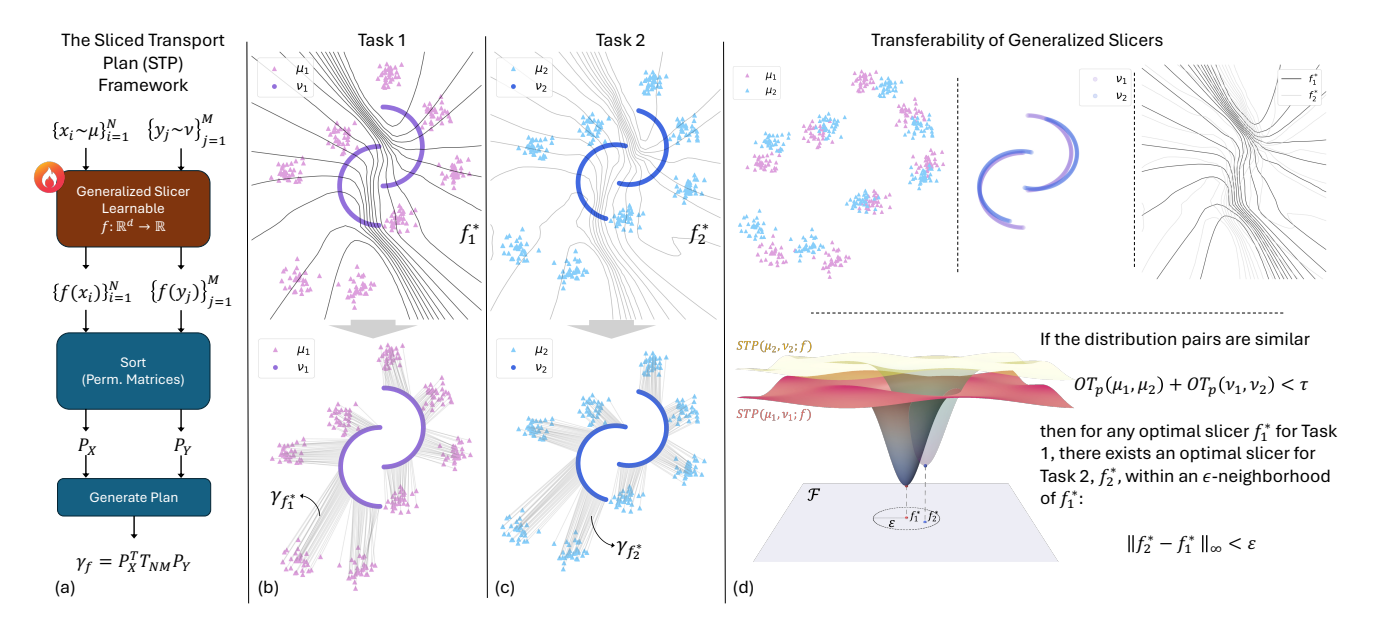


Figure 1. Overview of the Sliced Transport Plan (STP) framework and our transferability results. (a–c) The STP framework computes transport plans  $\gamma_f$  using a generalized slicer  $f:\mathbb{R}^d\to\mathbb{R}$ , which projects high-dimensional samples onto one-dimensional marginals, sorts them via (soft) permutation matrices, and generates slice-wise transport plans that are lifted back to the ambient space to obtain a transportation plan between the input measures. The min-STP framework extends STP by learning an optimal slicer  $f^*$  that minimizes the transportation cost in the ambient space. (d) In this paper, we establish a *transferability theorem* showing that if two source-target distribution pairs  $(\mu_1, \nu_1)$  and  $(\mu_2, \nu_2)$  are close, then there exists an optimal slicer  $f_2^*$  for  $(\mu_2, \nu_2)$  in an  $\varepsilon$ -vicinity of  $f_1^*$ . This result enables efficient slicer reuse across related tasks, achieving amortized optimal transport.

pairs of distributions are nearly identical, current solvers recompute everything from scratch. This inefficiency is particularly limiting in domains such as developmental biology, where cell populations evolve gradually and successive distributions differ only slightly.

In this work, we move beyond isolated optimization and propose a formal framework for quantifying and leveraging the transferability of OT solutions. Our approach enables reusing information from previously solved instances, paving the way for adaptive, amortized OT across related problems. Building on differentiable generalized sliced plans [9], we revisit the min-generalized slice formulation and present a unified theoretical and algorithmic framework with numerically stable implementations. The *closed-form* quantile function of the sum of Laplace distributions (Lap-Sum) [42] forms the backbone of both the theoretical and computational aspects of our method, allowing for efficient and differentiable evaluation of one-dimensional transport plans. Our central contribution is a transferability theorem that establishes a formal link between distributional similarity and slicer proximity: when two source-target distribution pairs are similar, their optimal slicers are correspondingly close. To the best of our knowledge, this result provides the first theoretical foundation for amortized slicer reuse. Finally, we demonstrate that the slicer can be trained stochastically on mini-batches ( $n \ll N$ ), requiring only slice-and-sort operations on small subsets and enabling scalable optimization via stochastic gradient descent for large-scale datasets.

**Contributions.** We advance the theoretical foundations and practical scalability of large-scale OT problems through the following contributions:

- 1. Theoretically characterizing the transferability of optimized slicers under small source-target perturbations;
- 2. Deriving finite-sample statistical guarantees for slicers optimized using source-target mini-batches; and,
- 3. Demonstrating transferability via amortized min-STP on point cloud alignment and mean-flow generations.

# 2. Preliminaries

**Definition 2.1.** Optimal Transport (OT). Let  $\mathcal{X} \subseteq \mathbb{R}^d$  endowed with a metric  $c: \mathcal{X} \times \mathcal{X} \to \mathbb{R}$ . We use  $\mathcal{P}(\mathcal{X})$  to denote the set of Borel probability measures defined on  $\mathcal{X}$ , and  $\mathcal{P}_p(\mathcal{X})$  to denote the subset of probability measures with finite  $p^{th}$  moment  $(p \in [1, \infty))$ , i.e.,  $\mathcal{P}_p(\mathcal{X}) := \{\mu \in \mathcal{P}(\mathcal{X}) \mid \int_{\mathcal{X}} c^p(x, x_0) \mathrm{d}\mu(x) < \infty$ , for some  $x_0 \in \mathcal{X}\}$ . For  $\mu, \nu \in \mathcal{P}_p(\mathcal{X})$ , the optimal transport distance (aka the p-Wasserstein distance) is defined as:

$$\mathrm{OT}_p(\mu,\nu) \coloneqq \left(\inf_{\gamma \in \Gamma(\mu,\nu)} \int_{\mathcal{X} \times \mathcal{X}} c^p(x,y) \, \mathrm{d}\gamma(x,y)\right)^{\frac{1}{p}}, (1)$$

where  $\Gamma(\mu,\nu) := \{ \gamma \in \mathcal{P}_p(\mathcal{X} \times \mathcal{X}) \mid \pi_\#^1 \gamma = \mu, \ \pi_\#^2 \gamma = \nu \},$  $\pi^i$ 's denote the canonical projections, and  $f_\#\mu$  denotes the pushforward of  $\mu$  through f, which is formally defined as  $f_\#\mu(A) = \mu(f^{-1}(A))$  for any Borel subset  $A \subseteq \mathcal{X}$ .

For  $p \in [1, \infty)$ ,  $\mathrm{OT}_p$  defines a proper metric between  $\mu$  and  $\nu$ , with many favorable geometric characteristics.

A prominent computational paradigm in optimal transport is the sliced-OT framework [35], which leverages the efficiency of OT [5, 34] solvers on one-dimensional measures by computing the OT distances between the one-dimensional marginals of d-dimensional measures. Owing to the injectivity of the Radon transform and the Cramér-Wold theorem (probabilistic route) or the Fourier Slice theorem (analytic viewpoint), comparing these marginals defines a valid metric between the original d-dimensional measures [23, 30].

**Definition 2.2.** Sliced OT. Let  $f: \mathbb{R}^d \times \mathbb{S}^{d-1} \to \mathbb{R}$  defined by the scalar projection  $f(x,\theta) = \langle x,\theta \rangle$ , where  $\langle x,\theta \rangle$  denotes the standard inner product in  $\mathbb{R}^d$ . The sliced OT (SOT) problem between two probability measures  $\mu, \nu \in \mathcal{P}_p(\mathcal{X})$  is defined as:

$$SOT_p(\mu, \nu) := \left( \int_{\mathbb{S}^{d-1}} OT_p^p(f(\cdot, \theta)_{\#}\mu, f(\cdot, \theta)_{\#}\nu) d\sigma(\theta) \right)^{\frac{1}{p}},$$

where  $\sigma \in \mathcal{P}(\mathbb{S}^{d-1})$  is a probability measure with non-zero density everywhere on the d-dimensional unit sphere  $\mathbb{S}^{d-1}$ .

The notion of slicing was later extended to *generalized slices* by allowing  $f(\cdot,\theta):\mathbb{R}^d\times\mathbb{R}^{d'}\to\mathbb{R}$  to be a nonlinear parametric function. With a slight abuse of notation, we drop  $\theta$  and write f when unambiguous. Under suitable assumptions on f [10, 22], it has been shown that SOT defines a proper metric between measures  $\mu,\nu\in\mathcal{P}_p(\mathbb{R}^d)$ . Notably, extensive work has also been dedicated to the choice of  $\sigma$ , which is orthogonal to our discussion and, therefore, we do not discuss it in this paper [31–33].

#### 2.1. Sliced Transportation Plans

The central idea behind methods that estimate transportation plans via slicing is that the one-dimensional transportation plan between the pushforward measures  $f_{\#}\mu$  and  $f_{\#}\nu$ , can be lifted back to define a coupling in the original space, denoted by  $\gamma_f$ . Following [28], in the case of discrete measures and injective projections f, this lifting is straightforward: the unique one-dimensional optimal plan calculated in the sliced space,  $\sigma_f \in \Gamma(f_{\#}\mu, f_{\#}\nu)$ , corresponds directly to a valid transportation plan for the original measures,  $\gamma_f \in \Gamma(\mu, \nu)$ . To the best of our knowledge, this idea of lifting via injective projections was first introduced by Rowland et al. [36] as part of the Projected Wasserstein (PW) distance framework between empirical distributions

and was later adopted in the influential work of Mahey et al. [29]. When the projections  $f_{\#}\mu$  and  $f_{\#}\nu$  are not injective, however, the lifting becomes non-trivial and requires more careful handling, as discussed in [28].

**Definition 2.3.** Sliced transportation plan (STP). Let  $\gamma_f$  denote the transportation plan between discrete probability measures  $\mu, \nu \in \mathcal{P}_p(\mathbb{R}^d)$ , obtained by lifting the optimal 1D plan from slices via an injective map f defined on the supports of  $\mu$  and  $\nu$ . We define the sliced transportation plan dissimilarity between  $\mu$  and  $\nu$  as:

$$\mathrm{STP}_p(\mu, \nu; f) \coloneqq \left( \sum_{x \in \mathrm{supp}(\mu)} \sum_{y \in \mathrm{supp}(\nu)} c^p(x, y) \, \gamma_f(x, y) \right)^{\frac{1}{p}}.$$

For general measures  $\mu, \nu \in \mathcal{P}_p(\mathcal{X})$ , we formally write

$$\mathrm{STP}_p(\mu, \nu; f) \coloneqq \left( \int_{\mathcal{X} \times \mathcal{X}} c^p(x, y) \, \mathrm{d}\gamma_f(x, y) \right)^{\frac{1}{p}}$$

whenever  $\gamma_f$  is a well-defined lift coupling; that is, if  $\sigma_f$  denotes the unique optimal transport plan between  $f_{\#}\mu$  and  $f_{\#}\nu$ , then  $\gamma_f$  is the uniquely determined element of  $\Gamma(\mu,\nu)$  satisfying the property  $(f,f)_{\#}\gamma_f=\sigma_f$ . Such uniqueness is guaranteed, for instance, when f is injective.

When  $f(\cdot) = \langle \cdot, \theta \rangle$ , for a certain  $\theta \in \mathbb{S}^{d-1}$ , and the cost function is  $c(x,y) = \|x - y\|_p$ , STP<sub>p</sub> coincides with the Sliced Wasserstein Generalized Geodesics (SWGG) distance [29], recently generalized for general measures [43].

**Proposition 2.4.** ([9, Proposition 2]) Let  $\mu, \nu \in \mathcal{P}_p(\mathcal{X})$ . Let  $f: \mathcal{X} \to \mathbb{R}$  be an injective map on the supports of  $\mu$ , and  $\nu$ . Then, for  $p \geq 1$ ,  $\mathrm{STP}_p(\cdot, \cdot; f)$  is a distance on  $\mathcal{P}_p(\mathcal{X})$ .

Since  $\gamma_f$  is a valid coupling of  $\mu$  and  $\nu$ , though not necessarily optimal, the cost induced by  $\gamma_f$  upper bounds the infimum in equation 1, i.e.,

$$\mathrm{OT}_{p}(\mu, \nu) \leq \mathrm{STP}_{p}(\mu, \nu; f).$$

While  $\mathrm{STP}_p$  provides an upper bound for  $\mathrm{OT}_p$ , the gap between the two could be large due to the potential discrepancy between  $\gamma_f$  and an optimal transport plan  $\gamma^*$  for equation 1. This motivates the introduction of the min-STP $_p$ , which coincides with the min-SWGG [29] and Differentiable Generalized Sliced Wasserstein Plan (DGSWP) defined by [9] in specific cases.

**Definition 2.5.** min-STP<sub>p</sub>. Let  $\mu, \nu \in \mathcal{P}_p(\mathcal{X})$ . The minimum Sliced Transportation Plan (min-STP<sub>p</sub>) between  $\mu$  and  $\nu$  is defined as:

$$\min-\text{STP}_p(\mu,\nu) = \min_{f \in \mathcal{F}} \text{STP}_p(\mu,\nu;f), \qquad (2)$$

where  $\mathcal{F}$  is a class of parametric functions.

Clearly, min-STP $_p$  satisfies:

$$\mathrm{OT}_p(\mu, \nu) \leq \mathrm{min}\text{-}\mathrm{STP}_p(\mu, \nu) \leq \mathrm{STP}_p(\mu, \nu; f).$$

Moreover, if  $f: \mathcal{X} \to \mathbb{R}$  is injective on  $\mathcal{X} \subset \mathbb{R}^d$ , then min-STP<sub>p</sub> provides a pseudo-metric on  $\mathcal{P}_p(\mathcal{X})$   $(p \ge 1)$ .

#### 3. Method and Theoretical Results

#### 3.1. Transferability

We first discuss the transferability of optimal slicers  $f^*: \mathcal{X} \to \mathbb{R}$  in problem 2. We show that when the source and target distributions experience small variations, the corresponding optimal slicer varies only marginally. This stability property ensures that  $f^*$  can be reliably transferred as a prior for the varied distributions.

**Definition 3.1** (Perturbed slicers). Let  $\mathsf{Lap}_d(\eta^2\Sigma)$  denote the symmetric multivariate Laplace distribution on  $\mathbb{R}^d$  with mean 0 and covariance matrix  $\eta^2\Sigma$ , for a scale parameter  $\eta>0$  and a symmetric positive definite matrix  $\Sigma\in\mathbb{R}^{d\times d}$ . Given a measurable function  $f:\mathcal{X}\to\mathbb{R}$ , we define its perturbation by

$$g_{\xi_n,f}(x) := f(x) + \langle \xi_n, x \rangle$$
, where  $\xi_n \sim \mathsf{Lap}_d(\eta^2 \Sigma)$ .

Unless more than a single function f is involved, we will omit the subscript f and write  $g_{\xi_n}$ .

Throughout this paper,  $\Sigma$  stays fixed and we focus on varying scales  $\eta$ . This choice is motivated by LapSum [42], which applies Laplace perturbations for order-type smoothing, and it integrates naturally with LapSum's differentiable sorting mechanisms used in our implementations (see Section 3.2). Specifically, the perturbation ensures that, for any  $\mu \in \mathcal{P}(\mathcal{X})$ , with  $\mu$ -probability one, the projection  $g_{\xi_{\eta}}$  is injective on the support of  $\mu$  (see Lemma 7.3 in the Supplementary Material). This thereby enables the lift of a 1D coupling to the original space: Given  $\mu, \nu \in \mathcal{P}(\mathcal{X})$ , for each  $\sigma \in \Gamma((g_{\xi_{\eta}})_{\#}\mu, (g_{\xi_{\eta}})_{\#}\nu) \subset \mathcal{P}(\mathbb{R} \times \mathbb{R})$ , there exists one and only one (lifted) coupling  $\gamma \in \Gamma(\mu, \nu) \subset \mathcal{P}(\mathcal{X} \times \mathcal{X})$  such that  $(g_{\xi_{\eta}}, g_{\xi_{\eta}})_{\#}\gamma = \sigma$  (see Proposition 7.4 in the Supplementary Material).

Generalizing the classical projectors  $f(x,\theta) = \langle x,\theta \rangle$  while preserving some of their fundamental properties, our model class assumptions are as follows:

**Assumption 3.2** (Model class). Let  $(\mathcal{X}, c)$  be a compact metric space in  $\mathbb{R}^d$ , and let  $\mathcal{F}$  consist of all Lipschitz continuous functions  $f: \mathcal{X} \to \mathbb{R}$  with global Lipschitz constant L > 0, and uniformly bounded by M > 0, i.e.,  $\mathcal{F} := \{f \in C(\mathcal{X}) \mid Lip(f) \leq L, \|f\|_{\infty} \leq M\}$ , where Lip(f) denotes the Lipschitz constant of f.

Under these assumptions, the slicer family  $\mathcal{F}$  is compact in the uniform norm (as a consequence of the Arzelà–Ascoli

theorem; see Lemma 7.1 in the Supplementary Material). Thus, minimizers of regular functionals are attained over  $\mathcal{F}$ . In particular, we next introduce an objective obtained by applying Laplace perturbations to STP, which has better regularity properties and recovers STP in the limit as the perturbations vanish.

**Definition 3.3** (Expected lifted plan). Let  $\mu, \nu \in \mathcal{P}(\mathcal{X})$ , and  $f \in \mathcal{F}$  with perturbation  $g_{\xi_{\eta}}$  for some  $\eta > 0$ . Let  $\sigma_{\xi_{\eta}}$  denote the 1D optimal plan between  $(g_{\xi_{\eta}})_{\#}\mu$  and  $(g_{\xi_{\eta}})_{\#}\nu$ , with corresponding (unique) lifted coupling  $\gamma_{\xi_{\eta}} \in \Gamma(\mu, \nu)$ , such that  $(g_{\xi_{\eta}}, g_{\xi_{\eta}})_{\#}\gamma_{\xi_{\eta}} = \sigma_{\xi_{\eta}}$ . We define the expected lifted plan and the smoothed objective by

$$\bar{\gamma}_f^{(\eta)} := \mathbb{E}_{\xi_\eta} [\gamma_{\xi_\eta}],$$

$$J_\eta(\mu, \nu; f) := \int_{\mathcal{X}^2} c(x, y)^p \, \mathrm{d}\bar{\gamma}_f^{(\eta)}(x, y). \tag{3}$$

**Theorem 3.4.** [Properties]

- 1. Let  $\mu, \nu \in \mathcal{P}(\mathcal{X})$ ,  $f \in \mathcal{F}$ . Then,  $\lim_{\eta \to 0} J_{\eta}(\mu, \nu; f) = \text{STP}_{\eta}^{p}(\mu, \nu; f)$ .
- 2. Let  $\mu_1, \nu_1, \mu_2, \nu_2 \in \mathcal{P}(\mathcal{X})$ . Given  $\varepsilon > 0$ , there exists  $\tau > 0$  such that if  $\mathrm{OT}_p(\mu_1, \mu_2) + \mathrm{OT}_p(\nu_1, \nu_2) < \tau$ , then for every  $f_1^\star \in \arg\min_{f \in \mathcal{F}} J_\eta(\mu_1, \nu_1; f)$ , there exists  $f_2^\star \in \arg\min_{f \in \mathcal{F}} J_\eta(\mu_2, \nu_2; f)$  in the  $\varepsilon$  neighborhood of  $f_1^\star$ , i.e.,  $\|f_2^\star f_1^\star\|_{\infty} < \varepsilon$ .

For the first property, we refer to Proposition 7.7 in the Supplementary Material, which uses the following auxiliary inequalities: for  $f, g \in \mathcal{F}$ ,  $\kappa, \kappa' \in \mathcal{P}(\mathcal{X})$ , and  $\mu_i, \nu_i \in \mathcal{P}(\mathbb{R})$  with optimal couplings  $\gamma_i$ , i = 1, 2,

- $\operatorname{OT}_p(f_\#\kappa, f_\#\kappa') \leq L \cdot \operatorname{OT}_p(\kappa, \kappa')$
- $OT_p(f_\#\kappa, g_\#\kappa) \le ||f g||_{\infty}$
- $\operatorname{OT}_p^p(\gamma_1, \gamma_2) \leq \operatorname{OT}_p(\mu_1, \mu_2)^p + \operatorname{OT}_p(\nu_1, \nu_2)^p$  (see Lemmas 7.5 and 7.6 in the Supplementary Material).

The second property in Theorem 3.4 is transferability. It holds as an application of Berge's Maximum Theorem [2] using compactness of  $\mathcal{F}$  (Model Assumption 3.2) together with the continuity of  $J_{\eta}$ . Indeed, Proposition 7.8 in the Supplementary Material establishes that  $J_{\eta}$  is continuous as a function on  $(\mathcal{P}(\mathcal{X}) \times \mathcal{P}(\mathcal{X})) \times \mathcal{F}$ , and its proof relies on the three inequalities listed above. For an illustration, see Figure 1 (d). For a preliminary discussion on the relationship between  $\tau$  and  $\varepsilon$ , we refer the reader to the Supplementary Material.

#### 3.2. Smoothed Sorting (LapSum)

An essential step in minimizing the STP objective is computing the one-dimensional optimal transport plan on  $\mathbb{R}$ . In one dimension, the OT problem reduces to sorting, which is inherently non-differentiable. To enable gradient-based optimization, a differentiable variant of the STP framework was introduced in [9]. The authors proposed the differentiable generalized sliced transport plan (DGSWP), which

formulates the search for a sliced plan as a bilevel optimization problem and smooths the outer, non-differentiable STP objective by injecting Gaussian noise into the slice parameters and estimating gradients using Stein's lemma. While this yields a differentiable surrogate, it suffers in practice from high variance when naive Monte Carlo estimators are used, as noted by the authors in [9] and shown in Figure 2. To mitigate this, they employed control variates as a variance-reduction technique to stabilize training. Nevertheless, the computational overhead of repeatedly solving one-dimensional OT problems for every perturbed slicer remains a significant bottleneck.

We adopt a different approach to inject differentiability into the optimization. It aligns with the smooth surrogate  $J_{\eta}$  proposed in Definition 3.3 and avoids the extra cost of repeated 1-D OT problems. This is achieved by leveraging LapSum, the differentiable sorting algorithm introduced in [42].

Let  $x_1, \ldots, x_n$  denote n scalars in  $\mathbb{R}$  with the corresponding empirical cumulative distribution function (CDF)

$$\hat{F}_x(t) = \frac{1}{n} \sum_{i=1}^n \mathbf{1} \{ x_i \le t \}.$$

Then the rank of  $x_i$  and sorted k-th value can be written as  $r_i = n \hat{F}_x(x_i), \quad x_{(k)} = \hat{F}_x^{-1}(k/n), \quad k = 1, \dots, n.$ 

LapSum injects i.i.d. Laplace noise  $\xi_i \sim \mathsf{Lap}(0, \alpha)$  and smooths each of the hard functions  $\mathbf{1}\{x_i \leq t\}$  as the CDF of  $\mathsf{Lap}(0, \alpha)$ , denoted by  $\Phi_{\alpha}$ , resulting in a smoothed CDF

$$\hat{F}_{x,\alpha}(t) = \frac{1}{n} \sum_{i=1}^{n} \Phi_{\alpha}(t - x_i).$$

This yields differentiable surrogates for rank and sorting:  $\tilde{r}_i = n\hat{F}_{x,\alpha}(x_i)$  and  $\tilde{x}_{(k)} = \hat{F}_{x,\alpha}^{-1}\left(\frac{k}{n}\right)$ , with  $\hat{F}_{x,\alpha} \to \hat{F}_x$  and  $\tilde{x}_{(k)} \to \operatorname{sort}(x)$  as  $\alpha \to 0$ . The elegance of LapSum is that the inverse  $\hat{F}_{x,\alpha}^{-1}$  can be calculated in closed-form and the algorithm has a complexity of only  $\mathcal{O}(n\log n)$  (see Algorithm 1 in [42] and the Supplementary Material for deriving LapSum-based soft permutation).

In our smooth surrogate in Definition 3.1, since the noise  $\xi \sim \operatorname{Lap}_d(\eta^2\Sigma)$ , each projection  $\langle \xi, x \rangle$  is a 1D Laplace distribution with scale  $b_x = \eta \sqrt{\frac{1}{2} \, x^\top \Sigma x}$  (see Lemma 7.2 in the Supplementary Material). In other words, we inject Laplacian noise into each of the one-dimensional samples and calculate the expectation of plans in one shot by Lap-Sum. This closely connects to the probabilistic assumptions of LapSum's soft comparisons. In practice, we conveniently adopt a fixed global scale for the Laplace noise across all samples, which allows for absorbing the perturbations in the calculations of the 1D optimal transport plan using LapSum, notably with a time complexity of only  $\mathcal{O}(n \log n)$  and  $\mathcal{O}(n)$  memory requirement.

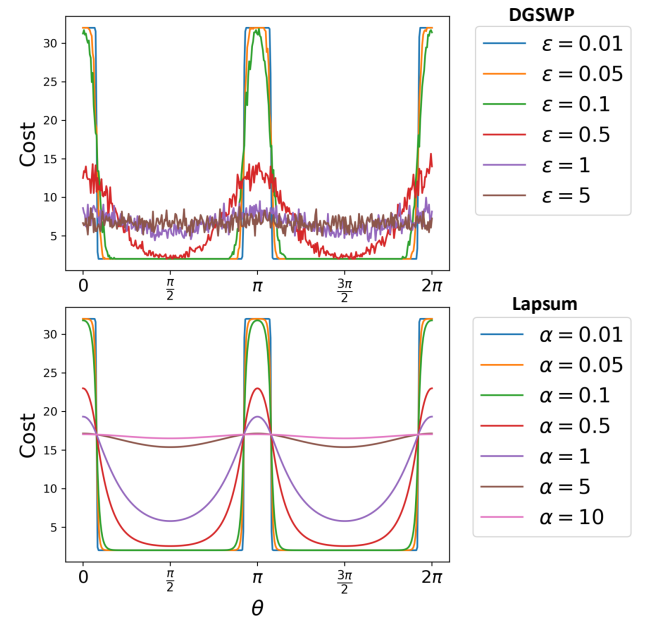


Figure 2. Transport costs with respect to slicing directions  $\theta \in \mathbb{S}^1$  for distribution pair  $\mu = \frac{1}{2}\delta_{[0,0]} + \frac{1}{2}\delta_{[1,1]}$  and  $\nu = \frac{1}{2}\delta_{[0,1]} + \frac{1}{2}\delta_{[1,0]}$ , using DGSWP [9] (50 perturbed samples) and LapSum[42]. LapSum yields smooth objectives across scales  $\alpha$ .

#### 3.3. Mini-batch Training

Training a slicer network on large-scale datasets is computationally demanding because each update requires evaluating the full STP objective. We mitigate this cost by optimizing a mini-batched STP loss, which enables fast iterations. Theoretically, we demonstrate that the gap between the full-batch and mini-batch objectives decays at a rate of  $\mathcal{O}(B^{-\frac{1}{2}})$ , where B represents the batch size.

Let  $X=\{x_i\}_{i=1}^N$  and  $Y=\{y_j\}_{j=1}^M$  be two sets of discrete samples, and define  $[n]:=\{1,\ldots,n\}$ . The discrete STP objective is given by  $J_{N,M}(f):=\sum_{i=1}^N\sum_{j=1}^M\gamma_{ij}\,c(x_i,y_j)^p$ , where  $\gamma$  denotes the lifted transport plan by  $f:\mathbb{R}^d\to\mathbb{R}$ . Fix a batch size  $B\le\min(N,M)$  and let  $\binom{[n]}{B}$  represent the set of all possible batches of B indices drawn from [n] without replacement. For  $S\in\binom{[N]}{B}$ ,  $T\in\binom{[M]}{B}$  and their corresponding batches  $x_S=(x_i)_{i\in S}$  and  $y_T=(y_j)_{j\in T}$ , define the kernel with slicer  $f:\mathbb{R}^d\to\mathbb{R}$  as

$$h_B(f; x_S, y_T) := \frac{1}{B} \sum_{i=1}^{B} c(x_{(i)}^f, y_{(i)}^f)^p,$$

where  $x_{(i)}^f, y_{(i)}^f \in \mathbb{R}^d$  denote the re-ordered  $x_S$  and  $y_T$ , paired by the lifted coupling from 1D coupling, i.e.,  $f(x_{(1)}^f) \leq \cdots \leq f(x_{(B)}^f)$  and  $f(y_{(1)}^f) \leq \cdots \leq f(y_{(B)}^f)$  for the slicer  $f: \mathbb{R}^d \to \mathbb{R}$ . The mini-batch STP loss is then

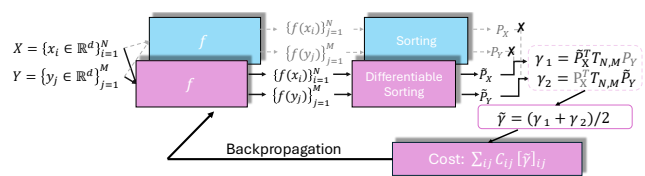


Figure 3. Training with two-branch symmetric gradients through differentiable sorting. The slicer f projects X and Y to one-dimensional samples that are (soft) sorted to obtain  $\tilde{P}_X$  and  $\tilde{P}_Y$  alongside hard permutations  $P_X, P_Y$ . Two plans are constructed,  $\gamma_1 = \tilde{P}_X^\top T_{N,M} P_Y$  and  $\gamma_2 = P_X^\top T_{N,M} \tilde{P}_Y$ , and the cost with their average is optimized  $\tilde{\gamma} = \frac{1}{2}(\gamma_1 + \gamma_2)$  via  $\sum_{i,j} c_{ij} [\tilde{\gamma}]_{ij}$ .

defined as

$$J_{N,M,B}(f) := \frac{1}{\binom{N}{B}\binom{M}{B}} \sum_{S \in \binom{[N]}{B}} \sum_{T \in \binom{[M]}{B}} h_B(f; x_S, y_T).$$

In practical implementations, the incomplete estimator draws K i.i.d. batch pairs  $\{(S_k, T_k)\}_{k=1}^K$  uniformly from  $\binom{[N]}{B} \times \binom{[M]}{B}$ , and averages:

$$\overline{J}_{B,K}(f) := \frac{1}{K} \sum_{k=1}^{K} h_B(f; x_{S_k}, y_{T_k}).$$

**Proposition 3.5.** For any  $\delta \in (0,1)$ , with probability at least  $1-\delta$ , there exist constants  $C_1, C_2, C_3, R$  (which depend on the datasets and f) such that

$$\left| \overline{J}_{B,K}(f) - J_{N,M}(f) \right| \le \frac{C_1}{B} + C_2 \omega_X(\frac{1}{2} \sqrt{\frac{N-B}{NB}}) + C_3 \omega_Y(\frac{1}{2} \sqrt{\frac{M-B}{MB}}) + R \sqrt{\frac{\log(2/\delta)}{2K}}.$$

where  $\omega_X, \omega_Y$  denote the quantile moduli of  $f_{\#}\mu_N$  and  $f_{\#}\nu_M$ , which are non-decreasing, and satisfy  $\omega_X(0) = \omega_Y(0) = 0$ . If we further assume the CDFs of  $f_{\#}\mu_N$  and  $f_{\#}\nu_M$  are smoothed and admit positive density lower bounds, then

$$\left| \overline{J}_{B,K}(f) - J_{N,M}(f) \right| \le \mathcal{O}(B^{-1/2}) + \mathcal{O}(K^{-1/2}).$$

Proof sketch. The proof proceeds in two steps: (i) controlling the mini-batch bias  $|J_{N,M,B}(f)-J_{N,M}(f)|$  and (ii) controlling the Monte Carlo fluctuation over K batches  $|\overline{J}_{B,K}(f)-J_{N,M,B}(f)|$ . The first term is deterministically bounded by a  $\mathcal{O}(B^{-1})$  term from well-stratified batches, together with the quantile moduli  $\omega_X, \omega_Y$  capturing deviations from this ideal stratification. The second term utilizes the fact that  $\mathbb{E}\overline{J}_{B,K}(f)=J_{N,M,B}(f)$ . By the boundedness of finite discrete samples, applying Hoeffding's inequality gives the probabilistic bound  $\mathcal{O}(K^{-1/2})$ . With additional regularity assumptions,  $\omega_X$  and  $\omega_Y$  are Lipschitz, which sharpens the bound. Details can be found in Propositions 8.2 and 8.7 in the Supplementary Material.

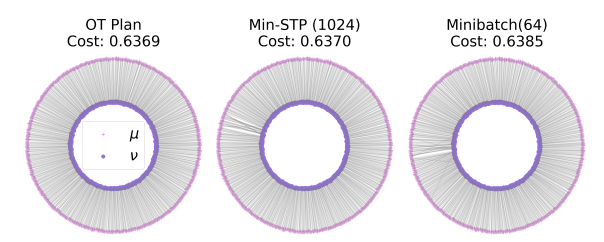


Figure 4. Transport plans and costs under different training schemes, along with the optimal plan/cost. Each panel visualizes pointwise correspondences (gray segments) between two ring distributions, source  $\mu$  and target  $\nu$ , with N=M=1024 points in each distribution. *left*: exact optimal transport (OT) plan. *middle*: min-STP trained with the full batch (all 1024 samples). *right*: mini-batch min-STP with batch sizes B=64.

# 3.4. Implementations

We train the slicer with symmetric two-branch gradient flows (see Figure 3). For the projected samples  $\{f(x_i)\}_{i=1}^N$  and  $\{f(y_j)\}_{j=1}^M$ , the differentiable LapSum operator produces soft permutation matrices  $\tilde{P}_X, \tilde{P}_Y$ . Let  $P_X, P_Y$  be the corresponding hard permutations and let  $T_{N,M} \in \mathbb{R}^{N \times M}$  be the fixed optimal transport plan between one-dimensional sorted N points and sorted M points. As differentiating through both soft permutations simultaneously may amplify noise and result in high variance in training, we form two plans during backpropagation,

$$\gamma_1 = \tilde{P}_X^\top T_{N,M} P_Y, \qquad \gamma_2 = P_X^\top T_{N,M} \tilde{P}_Y,$$

and optimize the loss using their average,  $\tilde{\gamma}:=\frac{1}{2}\left(\gamma_1+\gamma_2\right)$ , for more stable optimization. We empirically test the training scheme by comparing the transport plans produced by different training strategies, shown in Figure 4. The visualizations illustrate that the mini-batch min-STP maintains high-quality matching even for smaller batch sizes, closely resembling both the optimal transport plan and the full-batch min-STP solution.

# 4. Empirical Results

#### 4.1. Transferability under Gradual Drift

We evaluate slicer transferability on a sequence of gradually changing distribution pairs  $\{(\mu_t, \nu_t)\}_{t=1}^7$  generated from a fixed two-moons plus eight-Gaussians template in  $\mathbb{R}^2$ . Each distribution has 256 samples. In each step, we apply a small rotation and zoom-out to produce the next distribution pair. For every task, we use a Set-Transformer [27] as the parameterized slicer to minimize the STP objective. For  $t \geq 2$ , we compare initial values of the STP objective under two initializations: (i) **random initializations** (fresh and random parameters), and (ii) **transferred / pretrained initializations**, which reuses the optimal slicer  $f_{t-1}^{\star}$  from the previous task  $(\mu_{t-1}, \nu_{t-1})$ . As a lower bound, we also compute the OT cost between  $(\mu_t, \nu_t)$ .

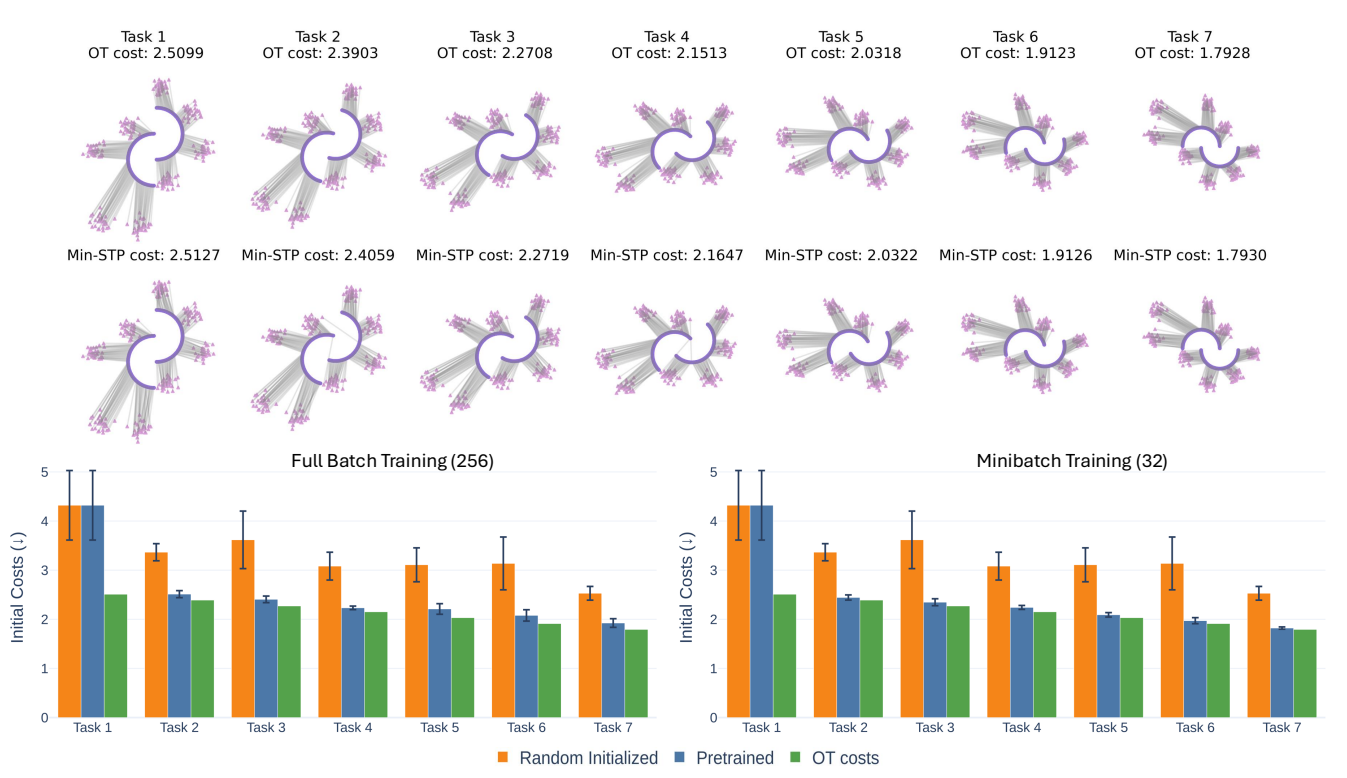


Figure 5. (Top row) The generated tasks  $\{(\mu_t, \nu_t)\}_{t=1}^7$  along with OT plans and costs. (Middle row) min-STP plans and costs optimized using the slicer with set transformer [27] architecture and pretrained weights. Pretraining refers to using the optimal slicer  $f_{t-1}^{\star}$  from the previous task  $\mu_{t-1}, \nu_{t-1}$  for  $t \geq 2$ . (Bottom row) *Initial* costs (averaging over 5 runs) of the slicer network against the OT lower bound, for both full batch training (left) and mini-batch training (right). The pretrained slicer begins near the OT cost, whereas the random slicer begins higher, confirming the transferability of the slicer. All values in the bar plots are measured *before* any optimization on task t. The cost for complete training is logged in Figure 11 in the Supplementary Material.

Figure 5 shows that in all steps, the pretrained initialization starts from a substantially lower objective than random and sits noticeably closer to the OT reference, indicating that leveraging  $f_{t-1}^{\star}$  places us at a much stronger starting point for the new task and the learned slicer captures geometry that persists under small rotations and scale changes.

#### 4.2. Amortized Min-STP for Point Cloud Alignment

To further assess the transferability of min-STP, we investigate whether a single amortized slicer can generalize across a family of related distribution pairs. We use the ModelNet10 dataset [47], which contains ten object categories (bathtub, bed, chair, desk, dresser, monitor, night\_stand, sofa, table, toilet), each represented as a point cloud of size 1024. For every ordered pair of categories, we construct training and test sets of distribution pairs by sampling point clouds from the corresponding classes. A single amortized slicer  $f_a^{\star}$  is then learned by minimizing a global objective over all training pairs. The slicer is implemented as an MLP with 3 hidden layers of dimensions [256, 512, 256]. As input, we concatenate each 3D point with a context vector, obtained from a pretrained point cloud auto-encoder. More details can be found in Section 9. We then compare the transport costs induced by  $f_a^{\star}$  with the exact OT costs and

against per-pair min-STP, STP with a random slicer, and Wasserstein Wormhole [19] as a global embedding from point clouds into a Euclidean space, trained to preserve pairwise Wasserstein distances.

Table 1 summarizes the mean and standard deviation of the Pearson correlations across category pairs. Figure 6 plots the correlations for a specific category pair: desk and sofa. More pairs can be found in Figure 12 in the Supplementary Material. Amortized min-STP achieves correlations with OT that are comparable to per-pair min-STP, which remains the upper bound since it optimizes a separate slicer for each pair. Amortized min-STP also consistently outperforms the two other baselines on both training and test pairs, indicating that a single slicer can effectively generalize across distributions.

#### 4.3. Min-STP based Flow

A promising application of optimal transport is its use in improving flow-based generative modeling [44] and single-step generation [24]. OT-MF [1] demonstrates that incorporating optimal transport into the MeanFlow algorithm [14] can enhance single-step generation performance across various tasks. Motivated by these findings, we aim to investigate the effectiveness of min-STP in a flow-based setting.

Table 1. Mean and standard deviation of Pearson correlations with exact OT over all ModelNet10 category pairs. Amortized min-STP matches per-pair min-STP and outperforms the baselines. Note that unlike STP-based methods Wasserstein Wormhole does not produce a transportation plan.

Method	Train Corr.	Test Corr.
min-STP (Amortized)	$0.907^{\pm0.048}$	$0.902^{\pm0.054}$
min-STP	$0.959^{\pm0.046}$	$0.947^{\pm0.073}$
STP (Random Slicer)	$0.702^{\pm0.090}$	$0.719^{\pm0.113}$
Wasserstein Wormhole	$0.831^{\pm0.132}$	$0.770^{\pm0.177}$

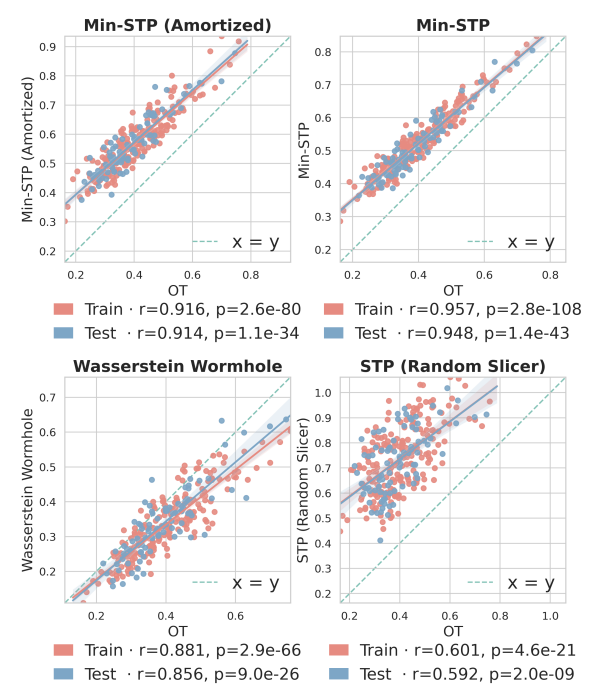


Figure 6. Correlations for desk and sofa pairs in Model-Net10. Amortized min-STP matches the performance of per-pair min-STP and outperforms the two other baselines.

Specifically, we adopt the experimental setup and datasets from [1] for point cloud generation, using ModelNet10 [47] and the "Chair" class from the ShapeNet dataset [8].

First, we train a slicer for each dataset using a Set-Transformer [26] architecture with two self-attention blocks (SAB) in both the encoder and decoder. During training, we treat each point cloud as an individual target distribution and use an isotropic Gaussian as the source distribution. Similar to Section 4.2, we obtain a context vector from the latent space of a pretrained autoencoder and concatenate it with all source and target points. Once the slicer is trained, we integrate it into the OT-MeanFlow framework to obtain a transport plan for each mini-batch. We follow the training setup and baselines provided in [1], and all experiments use single-step generation (NFE = 1). Figure 7 shows the average time required to compute OT per epoch vs. the 2-

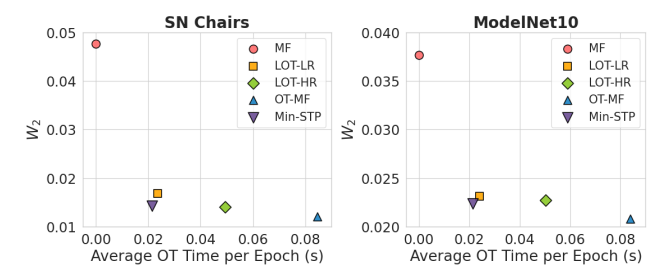


Figure 7. Average OT compute time per epoch vs. the  $\mathrm{OT}_2(W_2)$  distance for each method. For both metrics, lower is better.

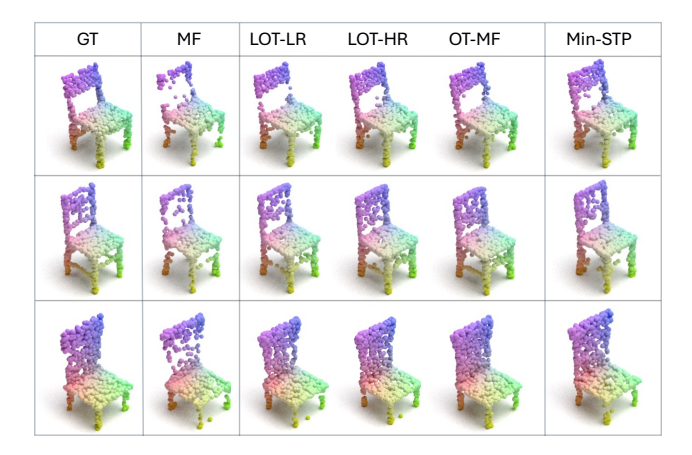


Figure 8. Single step sample generation on ShapeNet Chairs

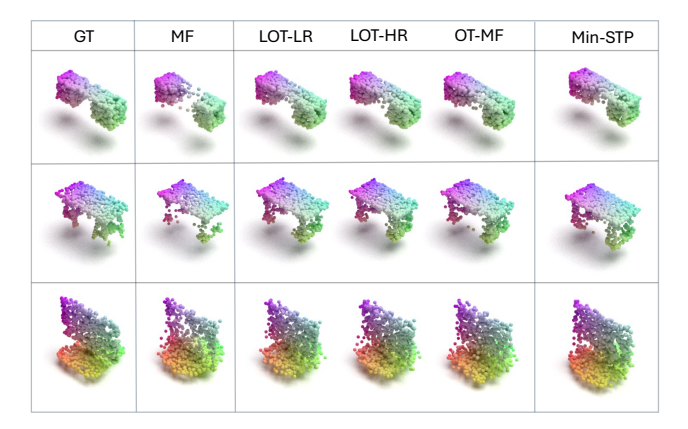


Figure 9. Single step sample generation on ModelNet10

Wasserstein distance  $(W_2)$  for min-STP and the baseline methods. A lower average  $W_2$  across test samples shows the ability of the method to generate point cloud samples that are closest to the ground truth. An ideal method should also achieve a lower computation time for OT to reduce the overall training cost.

As shown in Figure 7, min-STP appears in the bottomleft region of the plot, demonstrating its ability to balance low computation time with low  $W_2$ , resulting in higherquality generation with faster training. Figures 8 and 9 show generated samples (1-step) for ShapeNet-Chairs and ModelNet10, respectively. min-STP produces samples that more closely resemble the ground truth while adding only a slight overhead during training.

#### 5. Conclusion

We studied the transferability of optimized slicers in the min-Sliced Transport Plan (min-STP) framework. Leveraging smoothing via Laplace distributions, our theoretical results establish that optimal slicers are stable under small distributional shifts, hence enabling transfer across related source-target tasks. To improve scalability, we also introduced a mini-batch formulation of min-STP and provided guarantees for its approximation accuracy. We empirically showed that transferred slicers maintain strong performance in point cloud alignment and flow-based generative modeling, enabling efficient oneshot matching and amortized training. Our work highlights the promise of geometry-aware transport methods that generalize across domains and opens new avenues for scalable, transferable OT in dynamic, multi-domain settings.

#### References

- [1] Elaheh Akbari, Ping He, Ahmadreza Moradipari, Yikun Bai, and Soheil Kolouri. Transport based mean flows for generative modeling, 2025. 7, 8
- [2] Charalambos D Aliprantis and Kim C Border. *Infinite dimensional analysis: a hitchhiker's guide*. Springer, 2006. 4, 1, 5
- [3] Jason Altschuler, Jonathan Weed, and Philippe Rigollet. Near-linear time approximation algorithms for optimal transport via sinkhorn iteration. *Advances in Neural Information Processing Systems*, 2017. 1
- [4] Martin Arjovsky, Soumith Chintala, and Léon Bottou. Wasserstein generative adversarial networks. In *International conference on machine learning*, pages 214–223. PMLR, 2017.
- [5] Yikun Bai, Bernhard Schmitzer, Matthew Thorpe, and Soheil Kolouri. Sliced optimal partial transport. In *Proceedings of the IEEE/CVF Conference on Computer Vision and Pattern Recognition*, pages 13681–13690, 2023. 1, 3
- [6] Nicolas Bonneel, Julien Rabin, Gabriel Peyré, and Hanspeter Pfister. Sliced and Radon Wasserstein barycenters of measures. *Journal of Mathematical Imaging and Vision*, 51(1): 22–45, 2015. 1
- [7] Nicolas Bonnotte. *Unidimensional and evolution methods for optimal transportation*. PhD thesis, Université Paris Sud-Paris XI; Scuola normale superiore (Pise, Italie), 2013. 1
- [8] Angel X. Chang, Thomas Funkhouser, Leonidas Guibas, Pat Hanrahan, Qixing Huang, Zimo Li, Silvio Savarese, Manolis Savva, Shuran Song, Hao Su, Jianxiong Xiao, Li Yi, and Fisher Yu. Shapenet: An information-rich 3d model repository. arXiv preprint arXiv:1512.03012, 2015. 8
- [9] Laetitia Chapel, Romain Tavenard, and Samuel Vaiter. Differentiable generalized sliced Wasserstein plans. In *The*

- Thirty-ninth Annual Conference on Neural Information Processing Systems, 2025. 1, 2, 3, 4, 5
- [10] Xiongjie Chen, Yongxin Yang, and Yunpeng Li. Augmented sliced wasserstein distances. arXiv preprint arXiv:2006.08812, 2020. 3
- [11] Nicolas Courty, Rémi Flamary, Devis Tuia, and Alain Rakotomamonjy. Optimal transport for domain adaptation. *IEEE* transactions on pattern analysis and machine intelligence, 39(9):1853–1865, 2016. 1
- [12] Marco Cuturi. Sinkhorn distances: Lightspeed computation of optimal transport. Advances in neural information processing systems, 26:2292–2300, 2013. 1
- [13] Bharath Bhushan Damodaran, Benjamin Kellenberger, Rémi Flamary, Devis Tuia, and Nicolas Courty. Deepjdot: Deep joint distribution optimal transport for unsupervised domain adaptation. In *Proceedings of the European conference on computer vision (ECCV)*, pages 447–463, 2018. 1
- [14] Zhengyang Geng, Mingyang Deng, Xingjian Bai, J. Zico Kolter, and Kaiming He. Mean flows for one-step generative modeling. *arXiv* preprint arXiv:2505.13447, 2025. 7
- [15] Samuel Gerber and Mauro Maggioni. Multiscale strategies for computing optimal transport. *Journal of Machine Learn*ing Research, 18(72):1–32, 2017. 1
- [16] Ishaan Gulrajani, Faruk Ahmed, Martin Arjovsky, Vincent Dumoulin, and Aaron C Courville. Improved training of wasserstein gans. Advances in neural information processing systems, 30, 2017. 1
- [17] Wenxuan Guo, YoonHaeng Hur, Tengyuan Liang, and Chris Ryan. Online learning to transport via the minimal selection principle. In *Conference on Learning Theory*, pages 4085– 4109. PMLR, 2022.
- [18] Peter Halmos, Julian Gold, Xinhao Liu, and Benjamin Raphael. Hierarchical refinement: Optimal transport to infinity and beyond. In Forty-second International Conference on Machine Learning, 2025.
- [19] Doron Haviv, Russell Zhang Kunes, Thomas Dougherty, Cassandra Burdziak, Tal Nawy, Anna Gilbert, and Dana Pe'Er. Wasserstein wormhole: Scalable optimal transport distance with transformers. ArXiv, pages arXiv-2404, 2024.
- [20] Viet Huynh, He Zhao, and Dinh Phung. Otlda: A geometry-aware optimal transport approach for topic modeling. Advances in Neural Information Processing Systems, 33:18573–18582, 2020. 1
- [21] Abdelwahed Khamis, Russell Tsuchida, Mohamed Tarek, Vivien Rolland, and Lars Petersson. Scalable optimal transport methods in machine learning: A contemporary survey. *IEEE transactions on pattern analysis and machine intelli*gence, 2024. 1
- [22] Soheil Kolouri, Kimia Nadjahi, Umut Simsekli, Roland Badeau, and Gustavo Rohde. Generalized sliced Wasserstein distances. In Advances in Neural Information Processing Systems. Curran Associates, Inc., 2019. 3
- [23] Soheil Kolouri, Kimia Nadjahi, Shahin Shahrampour, and Umut Şimşekli. Generalized sliced probability metrics. In ICASSP 2022-2022 IEEE International Conference on Acoustics, Speech and Signal Processing (ICASSP), pages 4513–4517. IEEE, 2022. 1, 3

- [24] Nikita Kornilov, Petr Mokrov, Alexander Gasnikov, and Alexander Korotin. Optimal flow matching: Learning straight trajectories in just one step. arXiv preprint arXiv:2403.13117, 2024. 7
- [25] Nikita Kornilov, Petr Mokrov, Alexander Gasnikov, and Alexander Korotin. Optimal flow matching: Learning straight trajectories in just one step. In Advances in Neural Information Processing Systems, pages 104180–104204. Curran Associates, Inc., 2024. 1
- [26] Albert K Lee and Matthew A Wilson. Memory of sequential experience in the hippocampus during slow wave sleep. Neuron, 36(6):1183–1194, 2002. 8
- [27] Juho Lee, Yoonho Lee, Jungtaek Kim, Adam Kosiorek, Seungjin Choi, and Yee Whye Teh. Set transformer: A framework for attention-based permutation-invariant neural networks. In *International conference on machine learning*, pages 3744–3753. PMLR, 2019. 6, 7, 13
- [28] Xinran Liu, Rocio Diaz Martin, Yikun Bai, Ashkan Shah-bazi, Matthew Thorpe, Akram Aldroubi, and Soheil Kolouri. Expected sliced transport plans. In *The Thirteenth International Conference on Learning Representations*, 2025. 1, 3
- [29] Guillaume Mahey, Laetitia Chapel, Gilles Gasso, Clément Bonet, and Nicolas Courty. Fast optimal transport through sliced generalized wasserstein geodesics. Advances in Neural Information Processing Systems, 36:35350–35385, 2023. 1, 3
- [30] Kimia Nadjahi, Alain Durmus, Lénaïc Chizat, Soheil Kolouri, Shahin Shahrampour, and Umut Simsekli. Statistical and topological properties of sliced probability divergences. Advances in Neural Information Processing Systems, 33:20802–20812, 2020. 3
- [31] Khai Nguyen and Nhat Ho. Energy-based sliced wasserstein distance. In *Thirty-seventh Conference on Neural Information Processing Systems*, 2023. 3
- [32] Khai Nguyen, Nhat Ho, Tung Pham, and Hung Bui. Distributional sliced-wasserstein and applications to generative modeling. In *International Conference on Learning Representations*, 2021.
- [33] Khai Nguyen, Shujian Zhang, Tam Le, and Nhat Ho. Sliced wasserstein with random-path projecting directions. In *International Conference on Machine Learning*, pages 37879–37899. PMLR, 2024. 3
- [34] Gabriel Peyré and Marco Cuturi. Computational optimal transport: With applications to data science. *Foundations and Trends in Machine Learning*, 11(5-6):355–607, 2019. 1, 3
- [35] Julien Rabin, Gabriel Peyré, Julie Delon, and Marc Bernot. Wasserstein barycenter and its application to texture mixing. In *International Conference on Scale Space and Variational Methods in Computer Vision*, pages 435–446. Springer, 2011. 3
- [36] Mark Rowland, Jiri Hron, Yunhao Tang, Krzysztof Choromanski, Tamas Sarlos, and Adrian Weller. Orthogonal estimation of wasserstein distances. In *The 22nd International Conference on Artificial Intelligence and Statistics*, pages 186–195. PMLR, 2019. 1, 3
- [37] Mahdi Saleh, Shun-Cheng Wu, Luca Cosmo, Nassir Navab, Benjamin Busam, and Federico Tombari. Bending graphs:

- Hierarchical shape matching using gated optimal transport. In *Proceedings of the IEEE/CVF Conference on Computer Vision and Pattern Recognition*, pages 11757–11767, 2022.
- [38] Meyer Scetbon. Low-rank optimal transport: Approximation, statistics and debiasing. In Advances in Neural Information Processing Systems. 1
- [39] Geoffrey Schiebinger, Jian Shu, Marcin Tabaka, Brian Cleary, Vidya Subramanian, Aryeh Solomon, Joshua Gould, Siyan Liu, Stacie Lin, Peter Berube, et al. Optimal-transport analysis of single-cell gene expression identifies developmental trajectories in reprogramming. *Cell*, 176(4):928–943, 2019. 1
- [40] Bernhard Schmitzer. A sparse multiscale algorithm for dense optimal transport. *Journal of Mathematical Imaging and Vision*, 56(2):238–259, 2016.
- [41] Zhengyang Shen, Jean Feydy, Peirong Liu, Ariel H Curiale, Ruben San Jose Estepar, Raul San Jose Estepar, and Marc Niethammer. Accurate point cloud registration with robust optimal transport. Advances in Neural Information Processing Systems, 34:5373–5389, 2021. 1
- [42] Lukasz Struski, Michal B. Bednarczyk, Igor T. Podolak, and Jacek Tabor. Lapsum - one method to differentiate them all: Ranking, sorting and top-k selection. In Forty-second International Conference on Machine Learning, 2025. 2, 4, 5, 15
- [43] Eloi Tanguy, Laetitia Chapel, and Julie Delon. Sliced optimal transport plans. arXiv preprint arXiv:2508.01243, 2025.
- [44] Alexander Tong, Kilian FATRAS, Nikolay Malkin, Guillaume Huguet, Yanlei Zhang, Jarrid Rector-Brooks, Guy Wolf, and Yoshua Bengio. Improving and generalizing flowbased generative models with minibatch optimal transport. *Transactions on Machine Learning Research*, 2024. Expert Certification. 7
- [45] Cedric Villani. Optimal transport: old and new. Springer, 2009. 1
- [46] Wei Wang, Dejan Slepčev, Saurav Basu, John A Ozolek, and Gustavo K Rohde. A linear optimal transportation framework for quantifying and visualizing variations in sets of images. *International journal of computer vision*, 101(2):254–269, 2013. 1
- [47] Zhirong Wu, Shuran Song, Aditya Khosla, Fisher Yu, Linguang Zhang, Xiaoou Tang, and Jianxiong Xiao. 3d shapenets: A deep representation for volumetric shapes. In Proceedings of the IEEE conference on computer vision and pattern recognition, pages 1912–1920, 2015. 7, 8, 14
- [48] Karren Dai Yang, Karthik Damodaran, Saradha Venkatachalapathy, Ali C Soylemezoglu, GV Shivashankar, and Caroline Uhler. Predicting cell lineages using autoencoders and optimal transport. *PLoS computational biology*, 16(4): e1007828, 2020.
- [49] Mikhail Yurochkin, Sebastian Claici, Edward Chien, Farzaneh Mirzazadeh, and Justin M Solomon. Hierarchical optimal transport for document representation. *Advances in neural information processing systems*, 32, 2019. 1

# Efficient Transferable Optimal Transport via Min-Sliced Transport Plans

# Supplementary Material

# 6. Transferability (Overview)

In this section, we present the five building blocks of our transferability framework, and in the next section we expand on each component in detail.

A high-level outline is as follows:

## 1. Model assumption and properties.

Assumption 3.2: Compact metric space  $\mathcal{X} \subset \mathbb{R}^d$  and bounded Lipschitz function class  $\mathcal{F}$ .

Lemma 7.1: By Arzelà–Ascoli,  $\mathcal{F}$  is compact in the space of continuous functions  $C(\mathcal{X})$  defined on  $\mathcal{X}$  with respect to the uniform convergence.

### 2. Perturbed version of STP.

#### 2.1 Definition of the perturbation noise.

Definition 3.1: Laplace perturbation  $\xi_{\eta} \sim \operatorname{Lap}_d(\eta^2 \Sigma)$ . Lemma 7.2: In one dimension,  $\langle \xi_{\eta}, x \rangle$  follows a univariate Laplace distribution with scale  $b_x = \eta \sqrt{\frac{1}{2} x^\top \Sigma x}$ .

# 2.2 Definition of the perturbed slicer: Injectivity $\rightarrow$ unique lifting.

Definition 3.1: Perturbed slicer  $g_{\xi_{\eta}}(x) := f(x) + \langle \xi_{\eta}, x \rangle$ . Lemma 7.3: Given  $\mu, \nu \in \mathcal{P}(\mathcal{X})$ , for almost every  $\xi_{\eta}$ , the perturbed slicer  $g_{\xi_{\eta}}(x) = f(x) + \langle \xi_{\eta}, x \rangle$  is  $\mu$ - and  $\nu$ -a.e. injective.

Proposition 7.4: For almost every  $\xi_{\eta}$ , the 1D optimal plan between  $(g_{\xi_{\eta}})_{\#}\mu$  and  $(g_{\xi_{\eta}})_{\#}\nu$  admits a unique lifted coupling in  $\Gamma(\mu,\nu)$ .

#### 2.3 Definition of the smoothed objective.

Definition 3.3: Expected lifted plan and corresponding smoothed objective

$$\bar{\gamma}_f^{(\eta)} = \mathbb{E}_{\xi_\eta}[\gamma_{\xi_\eta}], \ J_\eta(\mu, \nu; f) = \int c(x, y)^p \,\mathrm{d}\bar{\gamma}_f^{(\eta)}(x, y).$$

#### 2.4 Agreement with STP when perturbations vanish.

Proposition 7.7: if f is continuous and injective, then  $J_{\eta}(\mu,\nu;f) \to \mathrm{STP}_{p}^{p}(\mu,\nu;f)$  as  $\eta \to 0$ .

#### 3. Continuity of $J_{\eta}$ .

Auxiliary inequalities (Lemma 7.5, Lemma 7.6) to bound Wasserstein distances of pushforward measures and optimal couplings.

Proposition 7.8: If  $W_p(\mu_n, \mu) \to 0$ ,  $W_p(\nu_n, \nu) \to 0$ , and  $||f_n - f||_{\infty} \to 0$ , then  $J_{\eta}(\mu_n, \nu_n; f_n) \to J_{\eta}(\mu, \nu; f)$ .

# 4. Compactness and application of the Maximum Theorem.

Using the continuity of  $J_{\eta}$  and compactness of  $\mathcal{F}$ , Berge's Maximum Theorem [2] applies.

Proposition 7.12:

- $v(\mu, \nu) := \min_{f \in \mathcal{F}} J_{\eta}(\mu, \nu; f)$  is continuous in the product space of probability measures endowed with the product OT metric  $(\mathcal{P}(\mathcal{X}) \times \mathcal{P}(\mathcal{X}), OT_p + OT_p)$ ;
- The argmin correspondence  $S(\mu, \nu) := \arg\min_{f \in \mathcal{F}} J_{\eta}(\mu, \nu; f)$  defined a nonempty and compact set in  $(\mathcal{F}, \|\cdot\|_{\infty})$  for each  $(\mu, \nu) \in \mathcal{P}(\mathcal{X})$ , and it is an upper hemicontinuous set-value function.

#### 5. Transferability of the optimal slicer.

Theorem 7.13: If two input pairs  $(\mu_1, \nu_1)$ ,  $(\mu_2, \nu_2)$  are close in  $W_p$ , then any minimizer  $f_1^\star \in \mathcal{S}(\mu_1, \nu_1)$  has a nearby minimizer  $f_2^\star \in \mathcal{S}(\mu_2, \nu_2)$  with  $\|f_2^\star - f_1^\star\|_\infty < \varepsilon$ .

# 7. Transferability (In Detail)

#### 1. Model assumption and properties.

Under Assumption 3.2, we take  $\mathcal{X} \subset \mathbb{R}^d$  to be a compact metric space. Since  $\mathcal{X}$  is compact, all probability measures on  $\mathcal{X}$  automatically have finite p-th moments. Therefore,

$$\mathcal{P}_p(\mathcal{X}) = \mathcal{P}(\mathcal{X}).$$

**Lemma 7.1.** Consider the family  $\mathcal{F}$  defined over the compact metric space  $(\mathcal{X} \subset \mathbb{R}^d, d)$  under Assumption 3.2. Then  $\mathcal{F}$  is compact in  $(C(\mathcal{X}), \|\cdot\|_{\infty})$ .

*Proof.* For any  $\varepsilon > 0$ , choose  $\delta := \varepsilon/L$ . If  $d(x,y) < \delta$ , then for all  $f \in \mathcal{F}$ , we have  $|f(x) - f(y)| \leq Ld(x,y) < \varepsilon$ . By uniform boundedness,  $\|f\|_{\infty} < M$  for all  $f \in \mathcal{F}$ . For each  $x \in \mathcal{X}$ , the set  $\{f(x) : f \in \mathcal{F}\} \subset [-M,M]$  is compact. By Arzelà–Ascoli theorem on the compact space  $\mathcal{X}$ ,  $\mathcal{F}$  is precompact in  $\|\cdot\|_{\infty}$  (i.e., its closure is compact in the ambient space). Moreover,  $\mathcal{F}$  is closed as uniform limits preserve the Lipschitz constant L and the sup bound M. Therefore,  $\mathcal{F}$  is compact since  $C(\mathcal{X})$  is compact under the uniform topology.

#### 2. Perturbed version of STP.

We recall that a 1D random variable has a Laplace distribution  $\operatorname{Lap}_1(0,b)$  if its probability density function is  $\frac{1}{2b}e^{-\frac{|x|}{b}}$ . For the symmetric multivariate Laplace distribution  $\operatorname{Lap}_d(0,\Sigma)$  in  $\mathbb{R}^d$ , where  $\Sigma \in R^{d \times d}$  is a symmetric positive definite matrix, a typical characterization is given through its characteristic function:  $\left(1+\frac{1}{2}\ t^\top \Sigma t\right)^{-1}, t \in \mathbb{R}^d$ .

**Lemma 7.2** (Noisy perturbations are Laplace). Let  $\xi \sim \text{Lap}_d(\eta^2 \Sigma)$ . For any fixed  $x \in \mathbb{R}^d$ ,

$$\langle \xi, x \rangle \; \sim \; \mathsf{Lap}_1 \big( 0, \; b_x \big), \qquad b_x = \eta \, \sqrt{\tfrac{1}{2} \, x^\top \Sigma x}.$$

In particular, with  $\Sigma=2I_d$  one gets  $\langle \xi,x\rangle\sim {\rm Lap}_1(0,\eta\|x\|_2).$ 

*Proof.* The characteristic function of  $\xi$  is  $\phi_{\xi}(t) = \left(1 + \frac{1}{2}\eta^2 t^{\top} \Sigma t\right)^{-1}$ ,  $t \in \mathbb{R}^d$ . For  $Y := \langle \xi, x \rangle$ ,  $\phi_Y(t) = \phi_{\xi}(tx) = \left(1 + \frac{1}{2}\eta^2 t^2 x^{\top} \Sigma x\right)^{-1}$ , which is the characteristic function of a univariate Laplace with 0 mean and scale  $b_x = \eta \sqrt{(x^{\top} \Sigma x)/2}$ .

**Lemma 7.3** (Injectivity of projection). Fix  $\eta > 0$ ,  $\mu \in \mathcal{P}(\mathcal{X})$  and  $f \in \mathcal{F}$ . With  $g_{\xi_{\eta}}$  from Definition 3.1, for  $\mathsf{Lap}_d(\eta^2\Sigma)$ -a.e.  $\xi_{\eta}$ , we have

$$(\mu \otimes \mu) \Big( \{ (x, x') : x \neq x', g_{\xi_{\eta}}(x) = g_{\xi_{\eta}}(x') \} \Big) = 0.$$

Consequently,  $g_{\xi_{\eta}}$  is  $\mu$ -a.e. injective, i.e., there exist a Borel set  $A_{\xi_{\eta}} \subseteq \mathcal{X}$  with  $\mu(A_{\xi_{\eta}}) = 1$  such that  $g_{\xi_{\eta}}|_{A_{\xi_{\eta}}} : A_{\xi_{\eta}} \to g_{\xi_{\eta}}(A_{\xi_{\eta}})$  is injective.

Proof. Define

$$H_{\mu}(\xi_{\eta}) := \iint \mathbf{1}_{\{x \neq x'\}} \mathbf{1}_{\{g_{\xi_{\eta}}(x) = g_{\xi_{\eta}}(x')\}} d\mu(x) d\mu(x').$$

The set  $C:=\{(\xi_\eta,x,x')\mid x\neq x',\,g_{\xi_\eta}(x)=g_{\xi_\eta}(x')\}$  is Borel in  $\mathbb{R}^d\times\mathcal{X}\times\mathcal{X}$  as  $(\xi_\eta,x)\mapsto g_{\xi_\eta}(x)=f(x)+\langle \xi_\eta,x\rangle$  is continuous and the constraints defining C come from Borel sets via continuous preimages and intersections (indeed, the diagonal  $D:=\{(x,x')\in\mathcal{X}\times\mathcal{X}\mid x=x'\}$  is closed in  $\mathcal{X}\times\mathcal{X}$  and so it is  $U:=\{(u,u')\in\mathbb{R}^2\mid u=u'\}$  in  $\mathbb{R}^2$ ; thus  $C=\mathbb{R}^d\times D^c\cap F^{-1}(U)$ , where  $F(\xi_\eta,x,x'):=(g_{\xi_\eta}(x),g_{\xi_\eta}(x'))$ , is Borel). Thus the integrand  $\mathbf{1}_{\{x\neq x'\}}\mathbf{1}_{\{g_{\xi_\eta}(x)=g_{\xi_\eta}(x')\}}$  is measurable and Tonelli's theorem applies in the expectation:

$$\mathbb{E}_{\xi_{\eta}}[H_{\mu}] = \iint \mathbf{1}_{\{x \neq x'\}} \mathbb{P}(g_{\xi_{\eta}}(x) = g_{\xi_{\eta}}(x')) d\mu(x) d\mu(x')$$

where  $\mathbb P$  denotes the probability of  $\operatorname{Lap}_d(\eta^2\Sigma).$  For fixed  $x\neq x',$ 

$$g_{\xi_n}(x) = g_{\xi_n}(x') \iff \langle \xi_n, x - x' \rangle = f(x') - f(x),$$

which is an affine hyperplane in  $\mathbb{R}^d$ , which has Lebesgue (hence  $\operatorname{Lap}_d(\eta^2\Sigma)$ ) measure 0. Therefore,  $\mathbb{E}_{\xi_\eta}[H_\mu]=0$  and, since  $H_\mu\geq 0$ , we get  $H_\mu(\xi_\eta)=0$  for a.e.  $\xi_\eta$ . Therefore  $(\mu\otimes\mu)\big(\big\{(x,x'):\ x\neq x',\ g_{\xi_\eta}(x)=g_{\xi_\eta}(x')\,\big\}\big)=0$  holds for a.e.  $\xi_\eta$ .

Now fix  $\xi_{\eta}$  such that  $H_{\mu}(\xi_{\eta}) = 0$ . Let  $\alpha_{\xi_{\eta}} := (g_{\xi_{\eta}})_{\#}\mu$ . Since  $\mathcal{X}$  and  $\mathbb{R}$  are standard Borel and  $g_{\xi_{\eta}}$  is Borel, Rokhlin's disintegration theorem provides a measurable family  $\{\mu_{u}\}_{u\in\mathbb{R}}$  with

$$\mu(B) \ = \ \int \mu_u(B) \, \mathrm{d}\alpha_{\xi_\eta}(u), \quad \forall B \text{ Borel},$$
 
$$\mu_u\!\left(\{x \mid \ g_{\xi_\eta}(x) = u\}\right) = 1 \quad \text{for } \alpha_{\xi_\eta}\text{-a.e. } u.$$

Write  $C_{\xi_{\eta}} := \{(x, x') \mid x \neq x', g_{\xi_{\eta}}(x) = g_{\xi_{\eta}}(x')\}$ . By definition of  $H_{\mu}$  and the disintegration,

$$0 = H_{\mu}(\xi_{\eta})$$

$$= (\mu \otimes \mu)(C_{\xi_{\eta}})$$

$$= \int (\mu_{u} \otimes \mu_{u}) (\{(x, x') \mid x \neq x'\}) d\alpha_{\xi_{\eta}}(u).$$

Hence, for  $\alpha_{\xi_n}$ -a.e. u,

$$(\mu_u \otimes \mu_u) \big( \{ (x, x') \mid x \neq x' \} \big) = 0.$$

We use the elementary fact: for a probability measure  $\rho$  on a standard Borel space,

$$(\rho \otimes \rho) \big( \{ (x, x') \mid x \neq x' \} \big) = 0 \iff \rho \text{ is a Dirac mass}$$

(indeed, if  $\rho$  is not Dirac, pick disjoint Borel sets B, B' with  $\rho(B), \rho(B') > 0$ , then  $(\rho \otimes \rho)(B \times B') > 0$ ). Therefore,  $\mu_u = \delta_{x_u}$  for  $\alpha_{\xi_\eta}$ -a.e. u, with  $x_u \in g_{\xi_\eta}^{-1}(\{u\})$ . Indeed, let  $S := \{u \in g_{\xi_\eta}(\mathcal{X}) \mid \mu_u \text{ is a Dirac Delta} \}$  then,  $\alpha_{\xi_\eta}(S) = 1$  and also, S is Borel as  $u \mapsto (\mu_u \otimes \mu_u)(\{x \neq x'\})$  is measurable. By the Jankov-von Neumann uniformization theorem we may choose the selector  $r: u \mapsto x_u$ , Borel on S. Define

$$A_{\xi_n} := r(S) = \{ x_u \in \mathcal{X} : u \in S \}.$$

Since r is Borel and injective between Borel spaces,  $A_{\xi_\eta}$  is Borel and

$$\mu(A_{\xi_{\eta}}) = \int \mu_u(A_{\xi_{\eta}}) d\alpha_{\xi_{\eta}}(u) = \int \mu_u(\{x_u\}) d\alpha_{\xi_{\eta}}(u)$$
$$= \int 1 d\alpha_{\xi_{\eta}}(u) = 1,$$

and if  $x_u, x'_{u'} \in A_{\xi_{\eta}}$  with  $u \neq u'$ , then  $g_{\xi_{\eta}}(x_u) = u \neq u' = g_{\xi_{\eta}}(x'_{u'})$ , while if u = u' the Dirac property forces  $x_u = x'_{u'}$ . Hence  $g_{\xi_{\eta}}|_{A_{\xi_{\eta}}}$  is injective.

**Proposition 7.4** (Uniqueness of the lift). Fix  $\eta > 0$ ,  $\mu, \nu \in \mathcal{P}(\mathcal{X})$  and  $f \in \mathcal{F}$ . Fix  $\xi_{\eta}$ ,  $g_{\xi_{\eta}}$  as in Definition 3.1 and set

$$\alpha_{\xi_{\eta}} := (g_{\xi_{\eta}})_{\#} \mu, \qquad \beta_{\xi_{\eta}} := (g_{\xi_{\eta}})_{\#} \nu.$$

Then for every  $\sigma \in \Gamma(\alpha_{\xi_n}, \beta_{\xi_n})$ , if  $\tilde{\gamma}, \hat{\gamma} \in \Gamma(\mu, \nu)$  satisfy

$$(g_{\xi_n}, g_{\xi_n})_{\#} \tilde{\gamma} = \sigma = (g_{\xi_n}, g_{\xi_n})_{\#} \hat{\gamma},$$

then  $\tilde{\gamma} = \hat{\gamma}$ .

*Proof.* Let  $A_{\xi_\eta}, B_{\xi_\eta}$  be Borel sets as in Lemma 7.3 with  $\mu(A_{\xi_\eta}) = 1 = \nu(B_{\xi_\eta})$  so that  $g_{\xi_\eta}|_{A_{\xi_\eta}} : A_{\xi_\eta} \to g_{\xi_\eta}(A_{\xi_\eta})$  and  $g_{\xi_\eta}|_{B_{\xi_\eta}} : B_{\xi_\eta} \to g_{\xi_\eta}(B_{\xi_\eta})$  are bijections with inverses  $j^{g_{\xi_\eta},\mu}, j^{g_{\xi_\eta},\nu}$ , respectively. By Lusin–Souslin theorem, such inverses are Borel measurable functions.

2

First note  $\tilde{\gamma}(A_{\xi_\eta} \times B_{\xi_\eta}) = 1 = \hat{\gamma}(A_{\xi_\eta} \times B_{\xi_\eta})$  because  $\mu(A_{\xi_\eta}) = \nu(B_{\xi_\eta}) = 1$ . Now, for any Borel  $E \subset A_{\xi_\eta} \times B_{\xi_\eta}$ , the map

$$(g_{\xi_\eta},g_{\xi_\eta})|_{A_{\xi_\eta}\times B_{\xi_\eta}}:\,A_{\xi_\eta}\times B_{\xi_\eta}\,\longrightarrow\,g_{\xi_\eta}(A_{\xi_\eta})\times g_{\xi_\eta}(B_{\xi_\eta})$$

is a Borel bijection with Borel inverse  $\Phi:=(j^{g_{\xi_\eta},\mu},j^{g_{\xi_\eta},\nu}).$  Hence

$$\tilde{\gamma}(E) = \tilde{\gamma} \left( \Phi \left( (g_{\xi_{\eta}}, g_{\xi_{\eta}})(E) \right) \right) = \sigma \left( (g_{\xi_{\eta}}, g_{\xi_{\eta}})(E) \right)$$

$$= \hat{\gamma} \left( \Phi \left( (g_{\xi_{\eta}}, g_{\xi_{\eta}})(E) \right) \right) = \hat{\gamma}(E),$$

where we used  $(g_{\xi_\eta},g_{\xi_\eta})_\# \tilde{\gamma} = \sigma = (g_{\xi_\eta},g_{\xi_\eta})_\# \hat{\gamma}$ . Therefore,  $\tilde{\gamma}$  and  $\hat{\gamma}$  coincide on  $A_{\xi_\eta} \times B_{\xi_\eta}$ . Since  $\tilde{\gamma}(A_{\xi_\eta} \times B_{\xi_\eta}) = \hat{\gamma}(A_{\xi_\eta} \times B_{\xi_\eta}) = 1$ , for any bounded Borel function  $\varphi$  on  $\mathcal{X}^2$ ,

$$\begin{split} \int \varphi \, \mathrm{d} \tilde{\gamma} &= \int \varphi \, \mathbf{1}_{A_{\xi_{\eta}} \times B_{\xi_{\eta}}} \, \mathrm{d} \tilde{\gamma} \\ &= \int \varphi \, \mathbf{1}_{A_{\xi_{\eta}} \times B_{\xi_{\eta}}} \, \mathrm{d} \hat{\gamma} = \int \varphi \, \mathrm{d} \hat{\gamma}. \end{split}$$

Thus, we conclude  $\tilde{\gamma} = \hat{\gamma}$ .

Notation: From now on, we will assume

$$c(x,y) = ||x - y||_p,$$

and for  $\mu, \nu \in \mathcal{P}(\mathcal{X})$  we write  $OT_p(\mu, \nu) = W_p(\mu, \nu)$  to refer to the *p*-Wasserstein distance defined in 1.

**Lemma 7.5.** For  $f, g \in \mathcal{F}$  and  $\kappa, \kappa' \in \mathcal{P}(\mathcal{X})$ ,

- $(1) W_p(f_\#\kappa, f_\#\kappa') \le L W_p(\kappa, \kappa')$
- (2)  $W_p(f_\#\kappa, g_\#\kappa) \le ||f g||_{\infty}$

*Proof.* (1) Let  $\gamma \in \Gamma(\kappa, \kappa')$  be any coupling between  $\kappa$  and  $\kappa'$ . Then  $(f, f)_{\#}\gamma \in \Gamma(f_{\#}\kappa, f_{\#}\kappa')$ , therefore

$$W_p^p(f_\#\kappa, f_\#\kappa') \le \int_{\mathbb{R}^2} |u - v|^p d((f, f)_\#\gamma)(u, v);$$

and by L-Lipschitzness,

$$\int_{\mathbb{R}^2} |u - v|^p d((f, f)_{\#}\gamma)(u, v)$$

$$= \int_{\mathcal{X}^2} |f(x) - f(y)|^p d\gamma(x, y)$$

$$\leq L^p \int_{\mathcal{X}^2} c(x, y)^p d\gamma(x, y).$$

Since this holds for any coupling  $\gamma \in \Gamma(\kappa, \kappa')$ ,

$$W_p^p(f_\#\kappa, f_\#\kappa') \le L^p \inf_{\gamma \in \Gamma(\kappa, \kappa')} \int_{\mathcal{X}^2} c(x, y)^p d\gamma(x, y)$$
$$= L^p W_p^p(\kappa, \kappa'),$$

which proves the claim (1).

(2) Consider the identity coupling  $\gamma_{id} \in \Gamma(\kappa, \kappa)$ . Then  $(f, g)_{\#} \gamma_{id} \in \Gamma(f_{\#} \kappa, g_{\#} \kappa)$  and

$$W_p^p(f_\#\kappa, g_\#\kappa) \le \int |f(x) - g(x)|^p \,\mathrm{d}\gamma_{id}(x, x)$$
$$= \int |f(x) - g(x)|^p \,\mathrm{d}\kappa(x) \le \|f - g\|_\infty^p.$$

Taking the p-th root gives the desired bound.

**Lemma 7.6.** For 1D probability measures  $\mu_i, \nu_i \in \mathcal{P}(\mathbb{R})$  with optimal couplings  $\gamma_i$ , i = 1, 2,

$$W_p(\gamma_1, \gamma_2) \le (W_p(\mu_1, \mu_2)^p + W_p(\nu_1, \nu_2)^p)^{1/p}$$

where the ground metric on  $\mathbb{R}^2$  is defined as  $\|(s,t) - (s',t')\|_p = (|s-s'|^p + |t-t'|^p)^{1/p}$  for  $s,t,s',t' \in \mathbb{R}$ .

*Proof.* Let  $Q_{\mu_i}$  and  $Q_{\nu_i}$  denote the quantile functions of  $\mu_i, \nu_i$ . Then the 1D p-Wasserstein distances between  $\mu_i$  and  $\nu_i$  are:

$$W_p^p(\mu_i, \nu_i) = \int_0^1 |Q_{\mu_i}(t) - Q_{\nu_i}(t)|^p dt,$$

and the corresponding optimal transport plan  $\gamma_i = (Q_{\mu_i}, Q_{\nu_i})_{\#} \lambda_{[0,1]}$ , where  $\lambda_{[0,1]}$  is the Lebesgue measure on [0,1]. Define  $\widetilde{\gamma} := (Q_{\mu_1}, Q_{\nu_1}, Q_{\mu_2}, Q_{\nu_2})_{\#} \lambda_{[0,1]} \in \Gamma(\gamma_1, \gamma_2)$ , then

$$\begin{split} W_p^p(\gamma_1, \gamma_2) &\leq \int_{(\mathbb{R}^2)^2} \|(u_1, v_1) - (u_2, v_2)\|_p^p \, \mathrm{d}\widetilde{\gamma} \\ &= \int_{(\mathbb{R}^2)^2} |u_1 - u_2|^p + |v_1 - v_2|^p \, \mathrm{d}\widetilde{\gamma} \\ &= \int_{[0,1]} |Q_{\mu_1}(s) - Q_{\mu_2}(s)|^p + |Q_{\nu_1}(s) - Q_{\nu_2}(s)|^p \, \mathrm{d}s \\ &= W_p^p(\mu_1, \mu_2) + W_p^p(\nu_1, \nu_2). \end{split}$$

Taking p-th root gives the claim.

**Proposition 7.7** (Recovery of STP as  $\eta \to 0$  for injective slicer). Assume  $f \in \mathcal{F}$  and **injective**. Let  $\alpha := f_{\#}\mu$ ,  $\beta := f_{\#}\nu$  and let  $\sigma_f$  be the 1D optimal coupling between  $\alpha$  and  $\beta$ . Define the (unique) lift  $\gamma_f \in \Gamma(\mu, \nu)$  such that

$$(f, f)_{\#} \gamma_f = \sigma_f,$$

and recall

$$STP_p^p(\mu,\nu;f) := \int_{\mathcal{X}^2} c(x,y)^p \,\mathrm{d}\gamma_f(x,y).$$

Let  $J_{\eta}(\mu, \nu; f)$  be the smoothed objective from Definition 3.3, then

$$\lim_{n\to 0} J_{\eta}(\mu,\nu;f) = STP_p^p(\mu,\nu;f).$$

*Proof.* Write  $\xi_{\eta}=\eta Z$  with  $Z\sim \mathsf{Lap}_d(\Sigma)$ , so that  $g_{\xi_{\eta}}(x)=f(x)+\eta\langle Z,x\rangle$ . For each instance Z, define the 1D marginals

$$\alpha_{\eta,Z} := (g_{\xi_{\eta}})_{\#}\mu, \qquad \beta_{\eta,Z} := (g_{\xi_{\eta}})_{\#}\nu,$$

and their optimal plan  $\sigma_{\eta,Z}$ . Let  $\gamma_{\eta,Z}$  be the (unique) lift of  $\sigma_{\eta,Z}$  given by Proposition 7.4:

$$(g_{\xi_{\eta}}, g_{\xi_{\eta}})_{\#} \gamma_{\eta, Z} = \sigma_{\eta, Z}, \qquad \gamma_{\eta, Z} \in \Gamma(\mu, \nu).$$

By Definition 3.3,  $J_{\eta}(\mu, \nu; f) = \mathbb{E}_{Z} \left[ \int c^{p}(x, y) \, d\gamma_{\eta, Z} \right]$ .

Since  $\mathcal X$  is compact, let  $R:=\sup_{x\in\mathcal X}\|x\|_p<\infty$ , and by Hölder's inequality,

$$||g_{\mathcal{E}_n} - f||_{\infty} \leq \eta ||Z||_q R;$$

where  $\frac{1}{p} + \frac{1}{q} = 1$ . By Lemma 7.5 part (2),

$$W_p(\alpha_{\eta,Z},\alpha) \leq \|g_{\xi_{\eta}} - f\|_{\infty} \leq \eta \|Z\|_q R,$$
  
similarly,  $W_p(\beta_{\eta,Z},\beta) \leq \eta \|Z\|_q R.$ 

Hence, as  $\eta \to 0$ , we have  $\alpha_{\eta,Z} \to \alpha$  and  $\beta_{\eta,Z} \to \beta$  in the one-dimensional  $W_p$ -distance for each fixed Z. By Lemma 7.6, as  $\eta \to 0$ , we have

$$W_p^p(\sigma_{\eta,Z},\sigma_f) \leq W_p^p(\alpha_{\eta,Z},\alpha) + W_p^p(\beta_{\eta,Z},\beta) \rightarrow 0,$$

for each fixed Z. Thus,  $\sigma_{\eta,Z} \rightharpoonup \sigma_f$  weakly as  $\eta \to 0$  (for each Z).

Let  $\eta_n \to 0$  with corresponding  $\{\gamma_{\eta_n,Z}\}_n$ . Since  $\mathcal{X}^2$  is compact,  $\mathcal{P}(\mathcal{X}^2)$  is also compact, and so there exists a subsequence  $\gamma_{\eta_{n_m},Z} \rightharpoonup \gamma^*$  for some probability measure  $\gamma^*$  on  $\mathcal{X}^2$ . For any bounded  $\varphi \in C(\mathbb{R}^2)$ ,

$$\int \varphi \, \mathrm{d}(g_{\xi_{\eta_{n_m}}}, g_{\xi_{\eta_{n_m}}})_{\#} \gamma_{\eta_{n_m}, Z}$$

$$= \int \varphi \left(g_{\xi_{\eta_{n_m}}}(x), g_{\xi_{\eta_{n_m}}}(y)\right) \, \mathrm{d}\gamma_{\eta_{n_m}, Z}(x, y)$$

$$= \int \varphi \, \mathrm{d}\sigma_{\eta_{n_m}, Z}.$$

Because  $g_{\xi_{\eta_{n_m}}} \to f$  uniformly on  $\mathcal X$  and  $\gamma_{\eta_{n_m},Z} \rightharpoonup \gamma^\star$ , the LHS tends to  $\int \varphi \big( f(x), f(y) \big) \, \mathrm{d} \gamma^\star(x,y)$ . The RHS tends to  $\int \varphi \, \mathrm{d} \sigma_f$ . Hence,

$$(f, f)_{\#} \gamma^{\star} = \sigma_f.$$

Since f is injective and continuous on compact  $\mathcal{X}$ , it is a continuous bijection from the compact space  $\mathcal{X}$  onto  $f(\mathcal{X}) \subset \mathbb{R}$  (Hausdorff), and so it is a homeomorphism: its inverse  $j^f: f(\mathcal{X}) \to \mathcal{X}$  is continuous. Then, the lift that solves  $(f,f)_\#\gamma = \sigma_f$  is unique and equals  $\gamma_f:=(j^f,j^f)_\#\sigma_f$ . In particular,  $\gamma^\star=\gamma_f$ . As the subsequence is arbitrary, we conclude that for each fixed Z,

$$\gamma_{\eta,Z} \rightharpoonup \gamma_f, \quad \text{as } \eta \to 0.$$

Thus, since  $c^p$  is bounded and continuous on the compact  $\mathcal{X}^2$ ,

$$\int c^p \, \mathrm{d}\gamma_{\eta,Z} \underset{\eta \to 0}{\longrightarrow} \int c^p \, \mathrm{d}\gamma_f \quad \text{for each fixed } Z.$$

Moreover,

$$0 \le \int c^p(x, y) \, \mathrm{d}\gamma_{\eta, Z}(x, y) \le (\mathrm{diam}(\mathcal{X}))^p < \infty,$$

so by Dominated Convergence (with respect to Z),

$$J_{\eta}(\mu, \nu; f) = \mathbb{E}_{Z} \Big[ \int c^{p} \, d\gamma_{\eta, Z} \Big] \xrightarrow{\eta \to 0} \mathbb{E}_{Z} \Big[ \int c^{p} \, d\gamma_{f} \Big]$$
$$= \int c^{p} \, d\gamma_{f}$$
$$= STP_{p}^{p}(\mu, \nu; f).$$

## 3. Continuity of $J_{\eta}$ .

**Proposition 7.8** (Continuity of  $J_{\eta}$ ). Fix  $\eta > 0$  and let  $J_{\eta}$  be given by Definition 3.3. If  $(\mu_n, \nu_n, f_n) \to (\mu, \nu, f)$  with  $W_p(\mu_n, \mu) \to 0$ ,  $W_p(\nu_n, \nu) \to 0$  and  $||f_n - f||_{\infty} \to 0$  (as  $n \to \infty$ ), then

$$J_{\eta}(\mu_n, \nu_n; f_n) \underset{n \to \infty}{\longrightarrow} J_{\eta}(\mu, \nu; f).$$

*Proof.* We write  $\xi_{\eta} = \eta Z$  with  $Z \sim \mathsf{Lap}_d(\Sigma)$ , and for each  $n \in \mathbb{N}$  and Z let

$$g_{n,Z}(x) := f_n(x) + \eta \langle Z, x \rangle, \quad g_Z(x) := f(x) + \eta \langle Z, x \rangle.$$

Set the 1D pushforwards

$$\alpha_{n,Z} := (g_{n,Z})_{\#} \mu_n, \qquad \beta_{n,Z} := (g_{n,Z})_{\#} \nu_n,$$
  
 $\alpha_Z := (g_Z)_{\#} \mu, \qquad \beta_Z := (g_Z)_{\#} \nu,$ 

and their optimal couplings  $\sigma_{n,Z}$  and  $\sigma_Z$ . By Lemma 7.3, for  $\mathbb{P}$ -a.e. Z, the lifts  $\gamma_{n,Z} \in \Gamma(\mu_n,\nu_n)$  and  $\gamma_Z \in \Gamma(\mu,\nu)$  are uniquely defined by

$$(g_{n,Z}, g_{n,Z})_{\#} \gamma_{n,Z} = \sigma_{n,Z}, \qquad (g_Z, g_Z)_{\#} \gamma_Z = \sigma_Z.$$

By Definition 3.3,

$$J_{\eta}(\mu_n, \nu_n; f_n) = \mathbb{E}_Z \left[ \int_{\mathcal{X}^2} c(x, y)^p \, d\gamma_{n, Z}(x, y) \right],$$
$$J_{\eta}(\mu, \nu; f) = \mathbb{E}_Z \left[ \int c^p \, d\gamma_Z \right].$$

Since  $f_n \to f$  uniformly and  $x \mapsto \langle Z, x \rangle$  is  $\|Z\|_q$ -Lipschitz (with 1/p+1/q=1), we have  $g_{n,Z} \to g_Z$  uniformly and  $\mathrm{Lip}(g_{n,Z}) \le L + \eta \|Z\|_q$ . By Lemma 7.5,

$$W_{p}(\alpha_{n,Z}, \alpha_{Z})$$

$$\leq W_{p}((g_{n,Z})_{\#}\mu_{n}, (g_{n,Z})_{\#}\mu) + W_{p}((g_{n,Z})_{\#}\mu, (g_{Z})_{\#}\mu)$$

$$\leq (L + \eta \|Z\|_{q}) W_{p}(\mu_{n}, \mu) + \|g_{n,Z} - g_{Z}\|_{\infty} \xrightarrow[n \to \infty]{} 0,$$

and similarly  $W_p(\beta_{n,Z},\beta_Z) \xrightarrow[n\to\infty]{} 0$ . By Lemma 7.6,

$$W_p(\sigma_{n,Z}, \sigma_Z) \le (W_p(\alpha_{n,Z}, \alpha_Z)^p + W_p(\beta_{n,Z}, \beta_Z)^p)^{1/p}$$

$$\xrightarrow[n \to \infty]{} 0 \quad \text{for each fixed } Z.$$

For each  $n\in\mathbb{N}_0$  (with n=0 denoting  $(\mu,\nu,f)$  and  $n\geq 1$  denoting  $(\mu_n,\nu_n,f_n)$ ), Lemma 7.3 yields a set  $G_n\subset\mathbb{R}^d$  with  $\mathbb{P}(Z\in G_n)=1$  such that  $g_{n,Z}$  is  $\mu_n$ -a.e. and  $\nu_n$ -a.e. injective for all  $Z\in G_n$ . Let  $G:=\bigcap_{n=0}^\infty G_n$ ; then  $\mathbb{P}(Z\in G)=1$  and all lifts above are defined uniquely for  $Z\in G$ .

Fix  $Z \in G$ . Since  $\mathcal{X}$  is compact, let  $\gamma_{n_m,Z} \rightharpoonup \bar{\gamma}$  be a convergent subsequence. Write  $\Phi_n(x,y) := (g_{n,Z}(x),g_{n,Z}(y))$  and  $\Phi(x,y) := (g_Z(x),g_Z(y))$ . Then  $\|\Phi_n - \Phi\|_{\infty} \to 0$ , and for any bounded function  $\varphi \in C(\mathbb{R}^2)$ .

$$\int \varphi \, \mathrm{d}\sigma_{n_m,Z} = \int \varphi \circ \Phi_{n_m} \, \mathrm{d}\gamma_{n_m,Z} \xrightarrow[m \to \infty]{} \int \varphi \circ \Phi \, \mathrm{d}\bar{\gamma},$$

while the LHS tends to  $\int \varphi \, \mathrm{d}\sigma_Z$ . Hence  $(g_Z,g_Z)_\# \bar{\gamma} = \sigma_Z$ . Since  $Z \in G$ ,  $g_Z$  is  $\mu$ -a.e. and  $\nu$ -a.e. injective, so the lift of  $\sigma_Z$  is *unique*; thus  $\bar{\gamma} = \gamma_Z$ . As the subsequence is arbitrary, the whole sequence converges:

$$\gamma_{n,Z} \rightharpoonup \gamma_Z \qquad (Z \in G).$$

In particular, since  $c^p$  is bounded and continuous on compact  $\mathcal{X}^2$ ,

$$\int c^p \, \mathrm{d}\gamma_{n,Z} \, \longrightarrow \, \int c^p \, \mathrm{d}\gamma_Z \qquad \text{for each } Z \in G.$$

Moreover,  $0 \leq \int c^p d\gamma_{n,Z} \leq (\operatorname{diam} \mathcal{X})^p$  for all n, Z. Hence, by dominated convergence (indeed, bounded convergence) with respect to Z,

$$J_{\eta}(\mu_{n}, \nu_{n}; f_{n}) = \mathbb{E}_{Z} \left[ \int c^{p} d\gamma_{n, Z} \right]$$

$$\underset{n \to \infty}{\longrightarrow} \mathbb{E}_{Z} \left[ \int c^{p} d\gamma_{Z} \right] = J_{\eta}(\mu, \nu; f).$$

# 4. Compactness and application of the Berge's Maximum Theorem.

We first review the Berge's Maximum Theorem [2].

**Definition 7.9** (Correspondence). A correspondence  $\varphi$  from a set X into a set Y assigns to each  $x \in X$  a subset  $\varphi(x)$  of Y ('point-to-set' assignment). We denote the correspondence as  $\varphi: X \rightrightarrows Y$ .

Just as functions have inverses, so do correspondences. Here, we are only concerned with a "strong inverse": For  $\varphi:X\rightrightarrows Y,$  the upper inverse  $\varphi^u$  or strong inverse is defined by

$$\varphi^u(A) = \{ x \in X \mid \varphi(x) \subset A \}.$$

Recall that a neighborhood of a set A is any set B for which there is an open set V satisfying  $A \subset V \subset B$ . Any open set V that satisfies  $A \subset V$  is called an *open neighborhood* of A.

**Definition 7.10** (Upper Hemicontinuity). A set-valued correspondence  $\varphi: X \rightrightarrows Y$  between topological spaces is upper hemicontinuous at the point x if for every open neighborhood U of  $\varphi(x)$ , the upper inverse image  $\varphi^u(U)$  is a neighborhood of x in X. As with functions, we say  $\varphi$  is upper hemicontinuous on X, abbreviated u.h.c., if it is upper hemicontinuous at every point of X.

**Theorem 7.11 (Berge's Maximum Theorem.).** Let  $\varphi: X \rightrightarrows Y$  be a continuous correspondence with nonempty compact values, and suppose  $f: X \times Y \to \mathbb{R}$  is continuous. Define the "value function"  $m: X \to \mathbb{R}$  by

$$m(x) := \sup_{y \in \varphi(x)} f(x, y),$$

and the correspondence  $\mu: X \rightrightarrows Y$  of maximizers by

$$s(x) \ := \ \{ \, y \in \varphi(x) \mid f(x,y) = m(x) \, \}.$$

Then, the value function m is continuous, and the "argmax" correspondence  $\mu$  is upper hemicontinuous with non-empty and compact values. As a consequence, the  $\sup$  may be replaced by  $\max$ .

**Proposition 7.12.** *Define the "argmin" correspondence* S :  $\mathcal{P}(\mathcal{X}) \times \mathcal{P}(\mathcal{X}) \to \mathcal{F}$ 

$$S(\mu, \nu) := \arg \min_{f \in \mathcal{F}} J_{\eta}(\mu, \nu; f),$$

and the minimum value function  $v: \mathcal{P}(\mathcal{X}) \times \mathcal{P}(\mathcal{X}) \to \mathbb{R}_{\geq 0}$ 

$$v(\mu,\nu) := \min_{f \in \mathcal{F}} J_{\eta}(\mu,\nu;f).$$

Then:

- 1. v is continuous on  $\Omega = (\mathcal{P}(\mathcal{X}) \times \mathcal{P}(\mathcal{X}), W_p + W_p)$ ;
- 2. for each  $\mu, \nu \in \mathcal{P}(\mathcal{X})$ , the set  $\mathcal{S}(\mu, \nu)$  is nonempty and compact (in  $\|\cdot\|_{\infty}$ );
- 3. S is upper hemicontinuous (u.h.c.) at every  $(\mu, \nu)$ .

*Proof.* By Proposition 7.8, the map  $J_{\eta}: \Omega \times \mathcal{F} \to \mathbb{R}$  is continuous on  $\Omega \times \mathcal{F}$ . As  $\mathcal{F}$  is non-empty and compact, applying Berge's Maximum Theorem 7.11 [2] with constant feasible correspondence  $\varphi(\mu,\nu) \equiv \mathcal{F}$ , the conclusion follows. Indeed, in the notation of Theorem 7.11, consider  $X = \mathcal{P}(\mathcal{X}) \times \mathcal{P}(\mathcal{X}), Y = \mathcal{F}, f = -J_{\eta}$ , and constant  $\varphi(\mu,\nu) = \mathcal{F}$  for each  $(\mu,\nu) \in X$ .

#### 5. Transferability of the optimal slicer.

**Theorem 7.13.** Given  $\varepsilon > 0$ , there exists  $\tau > 0$  such that if  $W_p(\mu_1, \mu_2) + W_p(\nu_1, \nu_2) < \tau$ , then for every  $f_1^\star \in \arg\min_{f \in \mathcal{F}} J_\eta(\mu_1, \nu_1; f)$ , there exists  $f_2^\star \in \arg\min_{f \in \mathcal{F}} J_\eta(\mu_2, \nu_2; f)$  in the  $\varepsilon$  neighborhood of  $f_1^\star$ , i.e.,  $\|f_2^\star - f_1^\star\|_{\infty} < \varepsilon$ .

*Proof.* Fix  $(\mu_2, \nu_2) \in \Omega$  and  $\varepsilon > 0$ . We will keep the notations in Proposition 7.12 and denote  $\mathcal{S}(\mu, \nu) := \arg \min_{f \in \mathcal{F}} J_{\eta}(\mu, \nu; f)$ . Consider the open neighborhood of  $\mathcal{S}(\mu_2, \nu_2)$ 

$$U_{\varepsilon} := \bigcup_{g \in \mathcal{S}(\mu_2, \nu_2)} \Big\{ f \in \mathcal{F} : \|f - g\|_{\infty} < \varepsilon \Big\}.$$

By upper hemicontinuity of S at  $(\mu_2, \nu_2)$  (Proposition 7.12 and the definition of u.h.c. for correspondences), there exists  $\tau > 0$  such that

$$d_{\Omega}((\mu_{1}, \nu_{1}), (\mu_{2}, \nu_{2})) = W_{p}(\mu_{1}, \mu_{2}) + W_{p}(\nu_{1}, \nu_{2}) < \tau$$
  
$$\Longrightarrow S(\mu_{1}, \nu_{1}) \subset U_{\varepsilon}.$$

Hence for any  $f_1^\star \in \mathcal{S}(\mu_1, \nu_1)$  there exists  $f_2^\star \in \mathcal{S}(\mu_2, \nu_2)$  such that  $\|f_2^\star - f_1^\star\|_{\infty} < \varepsilon$ .

# 7.1. Quantitative $\varepsilon$ - $\tau$ control.

We now quantify the  $\varepsilon$ - $\tau$  relation in Theorem 7.13. To do so, we make explicit how the smoothing scale  $\eta$  and a badevent with probability  $\delta$  come into play. For simplicity, assume p=2 and  $c(x,y)=\|x-y\|_2$ .

We expect that this analysis will motivate several directions for future research. Without appealing to the Berge's Maximum Theorem, we will show that can essentially say the following: For i=1,2, let

$$S_i := \arg\min_{f \in \mathcal{F}} J_{\eta}(\mu_i, \nu_i; f)$$

denote the set of minimizers, which are non-empty and compact under our assumptions. Given  $\varepsilon > 0$ , let  $U_{\varepsilon}(\mathcal{S}_i)$  denote the subset of functions in  $\mathcal{F}$  whose distance to  $\mathcal{S}_i$  is strictly less than  $\varepsilon$ . Consider the gaps

$$m_{\varepsilon}^{(i)} := \min_{f \in \mathcal{F} \setminus U_{\varepsilon}(\mathcal{S}_i)} J_{\eta}(\mu_i, \nu_i; f) - \min_{g \in \mathcal{F}} J_{\eta}(\mu_i, \nu_i; g).$$

Then if  $\mathcal{X}$  is finite, then with  $high\ probability$  one can choose  $\tau \leq m_{\varepsilon}^{(1)}/C$ , for a constant C depending on  $\eta$ , and obtain  $\mathcal{S}_2 \subset U_{\varepsilon}(\mathcal{S}_1)$ . Similarly, if  $\tau \leq m_{\varepsilon}^{(2)}/C$ , then  $\mathcal{S}_1 \subset U_{\varepsilon}(\mathcal{S}_2)$ , which in particular implies that for any  $f_1^* \in \mathcal{S}_1$ , there exists  $f_2 \in \mathcal{S}_2$  with  $\|f_2^* - f_1^*\|_{\infty} < \varepsilon$ .

Below we present the technical details, precisions, and future open directions.

**Assumption 7.14.** Let  $\Sigma = 2I_d$  and  $Z \sim \mathsf{Lap}_d(\Sigma)$ . We write  $\xi_{\eta} = \eta Z$  and slicers  $g_{\xi_{\eta}}(x) = f(x) + \eta \langle Z, x \rangle$  for  $f \in \mathcal{F}$ . To obtain a uniform inverse-Lipschitz bound for the slicers via a union bound, we will assume  $\mathcal{X}$  is finite with  $|\mathcal{X}| = B$ ; then there are  $B' = {B \choose 2}$  directions  $u_j \in \mathbb{S}^{d-1}$  associated with the pairs of elements in  $\mathcal{X}$ .

Step 1: A Lipschitz test for  $d^2(\cdot,\cdot)$ . First, let  $diam(\mathcal{X}) =: D < \infty$  (since, in general, we assume  $\mathcal{X}$  compact), and notice that the following inequalities

$$\begin{aligned} & \left| \left\| x_1 - y_1 \right\|_2^2 - \left\| x_2 - y_2 \right\|_2^2 \right| \\ &= \left| \left\langle (x_1 - y_1) + (x_2 - y_2), (x_1 - y_1) - (x_2 - y_2) \right\rangle \right| \\ &\leq \left( \left\| x_1 - y_1 \right\|_2 + \left\| x_2 - y_2 \right\|_2 \right) \left\| (x_1 - y_1) - (x_2 - y_2) \right\|_2 \\ &\leq 2D \left( \left\| x_1 - x_2 \right\|_2 + \left\| y_1 - y_2 \right\|_2 \right) \\ &\leq \underbrace{2\sqrt{2}D}_{=:D'} \sqrt{\left\| x_1 - x_2 \right\|_2^2 + \left\| y_1 - y_2 \right\|_2^2}_{=:D'} \\ &= D' \left\| (x_1, y_1) - (x_2, y_2) \right\|_2 \end{aligned}$$

imply that the function  $d^2/D': \mathbb{R}^d \times \mathbb{R}^d \to \mathbb{R}$  is 1-Lipschitz in  $\mathbb{R}^d \times \mathbb{R}^d$  with the standard Euclidean product metric. Thus, for any  $\gamma_1, \gamma_2 \in \mathcal{P}(\mathcal{X} \times \mathcal{X})$ , by using duality,

$$W_{2}(\gamma_{1}, \gamma_{2}) \geq W_{1}(\gamma_{1}, \gamma_{2})$$

$$= \sup_{Lip(\psi) \leq 1} \int \psi \, \mathrm{d}(\gamma_{1} - \gamma_{2})$$

$$\geq \frac{1}{D'} \int c(x, y)^{2} \, \mathrm{d}(\gamma_{1} - \gamma_{2}). \tag{4}$$

Step 2: Uniform inverse-Lipschitz for the slicers on a high-probability event. Now, we want to uniformly control the inverse-Lipschitz constant (or co-Lipschitz reciprocal) of the injective functions  $g_{\xi_{\eta}}$ . We recall that, for any fixed  $\eta>0$ , injectivity of the slicers  $g_{\xi_{\eta}}$  is guaranteed for a.e.  $\xi_{\eta}$  (Lemma 7.3), allowing us to later take  $\eta\to0$ . We fix  $\eta>0$ . For any distinct  $x,x'\in\mathcal{X}$ , let  $u:=(x-x')/\|x-x'\|_2\in\mathbb{S}^{d-1}$ , and from the reverse triangle inequality,

$$|g_{\xi_{\eta}}(x) - g_{\xi_{\eta}}(x')| \ge ||\langle \xi_{\eta}, x - x' \rangle| - |f(x) - f(x')||$$

$$\ge (\eta |\langle Z, u \rangle| - L) ||x - x'||_{2}.$$
 (5)

To beat the Lipschitz term L with high probability, we will use the extra assumptions 7.14:

1. 
$$\Sigma = 2I_d$$
,

2. 
$$|\mathcal{X}| = B < \infty$$
.

Assuming  $\Sigma=2I_d$ , by Lemma 7.2 one has  $\langle Z,u\rangle\sim {\sf Lap}_1(0,1)$  (i.e, we have isotropic variance –it does not depend on the direction u). Thus,

$$\mathbb{P}(|\langle Z, u \rangle| < t) = 1 - e^{-t}, \qquad t \ge 0.$$

The extra assumption of  $\mathcal X$  being **finite** with B number of elements, gives at most  $B'={B\choose 2}$  directions  $\{u_j\}_{j=1}^{B'}\subset$ 

 $\mathbb{S}^{d-1}$ . We can control  $\mathbb{P} \left( \min_{1 \leq j \leq B'} |\langle Z, u_j \rangle| < t \right)$  by the union bound  $\sum_{j=1}^{B'} \mathbb{P} (|\langle Z, u_j \rangle| < t) = B' (1 - e^{-t})$ . Let  $0 < \delta < 1$  such that  $t_{\delta,B} := -\ln \left( 1 - \frac{\delta}{B'} \right) > L/\eta$ . So,

$$\mathbb{P}\bigg(\underbrace{\min_{1 \leq j \leq B'} |\langle Z, u_j \rangle| \geq t_{\delta,B}}_{=:G \text{ ("good event")}}\bigg) \geq 1 - B' \big(1 - e^{-t_{\delta,B}}\big) =: 1 - \delta.$$

Hence, if we denote by  $K_Z$  the inverse-Lipschitz constant of  $g_{\xi_{\eta}}$ , from 5, on the "good event", with probability at least  $1-\delta$ , we get

$$K_Z \le \frac{1}{\eta t_{\delta,B} - L}.$$

In particular,

$$\sqrt{\mathbb{E}_Z(K_Z^2\mathbf{1}_G)} \le \frac{1}{\eta t_{\delta |B|} - L} \quad \text{with } \mathbb{P}(G) \ge 1 - \delta. \quad (6)$$

Therefore, the inverse-Lipschitz constant  $K_Z$  of the slicers  $g_{\xi_n}$  is globally bounded on a high-probability event G.

Step 3: Bound for the change of  $J_{\eta}$  with a fixed  $f \in \mathcal{F}$ . Given  $\mu_1, \mu_2, \nu_1, \nu_2 \in \mathcal{P}(\mathcal{X})$ , define  $\alpha_i^{(Z)} := (g_{\xi_{\eta}})_{\#} \mu_i$  and  $\beta_i^{(Z)} := (g_{\xi_{\eta}})_{\#} \nu_i$ . Let  $\sigma_i^{(Z)}$  be the *unique* 1D optimal plan between  $\alpha_i^{(Z)}, \beta_i^{(Z)}$ , with corresponding *unique* lifted coupling  $\gamma_i^{(Z)} \in \Gamma(\mu_i, \nu_i)$  such that  $(g_{\xi_{\eta}}, g_{\xi_{\eta}})_{\#} \gamma_i^{(Z)} = \sigma_i^{(Z)}$ , for i = 1, 2. Finally, define, as before,

$$J_{\eta}(\mu_i, \nu_i; f) := \int c(x, y)^p \,\mathrm{d}\bar{\gamma}_i^{(Z)}(x, y),$$

where  $\bar{\gamma}_i^{(Z)} = \mathbb{E}_Z[\gamma_i^{(Z)}]$  for i = 1, 2.

Using the above steps, for any  $f \in \mathcal{F}$ :

$$|J_{\eta}(\mu_{1}, \nu_{1}; f) - J_{\eta}(\mu_{2}, \nu_{2}; f)|$$

$$= \left| \mathbb{E}_{Z} \left( \int c(x, y)^{2} d(\gamma_{1}^{(Z)} - \gamma_{2}^{(Z)}) \right) \right|$$

$$\leq \mathbb{E}_{Z} \left( \left| \int c(x, y)^{2} d(\gamma_{1}^{(Z)} - \gamma_{2}^{(Z)}) \right| \mathbf{1}_{G} \right)$$

$$+ \mathbb{E}_{Z} \left( \left| \int c(x, y)^{2} d(\gamma_{1}^{(Z)} - \gamma_{2}^{(Z)}) \right| \mathbf{1}_{G^{c}} \right)$$

$$\leq \mathbb{E}_{Z} \left( \left| \int c(x, y)^{2} d(\gamma_{1}^{(Z)} - \gamma_{2}^{(Z)}) \right| \mathbf{1}_{G} \right)$$

$$+ 2 \operatorname{diam}(\mathcal{X})^{2} \delta.$$
(7)

Let us control the first term in 7: Using inequality 4 from Step 1, followed by Lemma 7.5 (part 1) with  $K_Z$  given from

Step 2, and then Lemma 7.6, we have

$$\mathbb{E}_{Z} \left( \left| \int c(x,y)^{2} d(\gamma_{1}^{(Z)} - \gamma_{2}^{(Z)}) \right| \mathbf{1}_{G} \right) \\
\leq D' \, \mathbb{E}_{Z} \left( W_{2}(\gamma_{1}^{(Z)}, \gamma_{2}^{(Z)}) \, \mathbf{1}_{G} \right) \\
\leq D' \, \mathbb{E}_{Z} \left( K_{Z} \, W_{2}(\sigma_{1}^{(Z)}, \sigma_{2}^{(Z)}) \, \mathbf{1}_{G} \right) \\
\leq D' \, \mathbb{E}_{Z} \left( K_{Z} \, \mathbf{1}_{G} (W_{2}^{2}(\alpha_{1}^{(Z)}, \alpha_{2}^{(Z)}) + W_{2}^{2}(\beta_{1}^{(Z)}, \beta_{2}^{(Z)}))^{\frac{1}{2}} \right) \\
\leq D' \, \mathbb{E}_{Z} \left( K_{Z} \, \mathbf{1}_{G} \left( L + \eta \|Z\|_{2} \right) \right) \left( W_{2}^{2}(\mu_{1}, \mu_{2}) + W_{2}^{2}(\nu_{1}, \nu_{2}) \right)^{\frac{1}{2}}.$$

We recall that the terms  $\left(W_2^2(\mu_1, \mu_2) + W_2^2(\nu_1, \nu_2)\right)^{\frac{1}{2}}$  and  $W_2(\mu_1, \mu_2) + W_2(\nu_1, \nu_2)$  are comparable, since

$$\sqrt{a^2 + b^2} \le a + b \le \sqrt{2}\sqrt{a^2 + b^2}$$
 for  $a, b > 0$ .

Moreover, by Cauchy-Schwartz inequality,

$$\mathbb{E}_{Z}(K_{Z}\mathbf{1}_{G}(L+\eta||Z||_{2}))$$

$$\leq (\mathbb{E}_{Z}(K_{Z}^{2}\mathbf{1}_{G}))^{\frac{1}{2}}(\mathbb{E}_{Z}((L+\eta||Z||_{2})^{2}))^{\frac{1}{2}}.$$

Again, by Cauchy-Schwartz inequality  $\mathbb{E}_Z(\|Z\|_2) \leq (\mathbb{E}_Z(\|Z\|_2^2))^{\frac{1}{2}}$ , and using  $\mathbb{E}_Z(\|Z\|_2^2) = \operatorname{tr}(\Sigma)$  one can estimate

$$\mathbb{E}_{Z}((L+\eta||Z||_{2})^{2}) \leq L^{2} + 2L\eta \operatorname{tr}(\Sigma)^{\frac{1}{2}} + \eta^{2} \operatorname{tr}(\Sigma)$$
$$= (L+\eta(\operatorname{tr}(\Sigma))^{\frac{1}{2}})^{2},$$

which, in particular, if  $\Sigma = 2I_d$ , then  $(\operatorname{tr}(\Sigma))^{\frac{1}{2}} = \sqrt{2d}$ . Therefore, replacing the above observations in 8 together with 6, we have

$$\mathbb{E}_{Z}\left(\left|\int c(x,y)^{2} d(\gamma_{1}^{(Z)} - \gamma_{2}^{(Z)})\right| \mathbf{1}_{G}\right)$$

$$\leq C(\eta, \delta) \left(W_{2}(\mu_{1}, \mu_{2}) + W_{2}(\nu_{1}, \nu_{2})\right),$$

where

$$C(\eta, \delta) := 2\sqrt{2} \operatorname{diam}(\mathcal{X}) \frac{L + \eta\sqrt{2d}}{\eta t_{\delta, B} - L}.$$
 (9)

As a conclusion,

$$|J_{\eta}(\mu_{1}, \nu_{1}; f) - J_{\eta}(\mu_{2}, \nu_{2}; f)|$$

$$\leq C(\eta, \delta) \left( W_{2}(\mu_{1}, \mu_{2}) + W_{2}(\nu_{1}, \nu_{2}) \right) + 2diam(\mathcal{X})^{2} \delta.$$
(10)

#### Step 4: From value stability to argmin transfer.

If  $W_2(\mu_1, \mu_2) + W_2(\nu_1, \nu_2) < \tau$ , inequality 10 implies

$$\left| \min_{f \in \mathcal{F}} J_{\eta}(\mu_1, \nu_1; f) - \min_{f \in \mathcal{F}} J_{\eta}(\mu_2, \nu_2; f) \right| < \underbrace{C(\eta, \delta)\tau + 2D^2 \delta}_{=:C'}$$

Indeed, if we define  $v_i := \min_{f \in \mathcal{F}} J_{\eta}(\mu_i, \nu_i; f)$ , and  $S_i := S(\mu_i, \nu_i) = \arg\min_{f \in \mathcal{F}} J_{\eta}(\mu_i, \nu_i; f)$  (non-empty

and compact), for i=1,2, from inequality 10 we have, in particular, that for any  $f_1^{\star} \in \mathcal{S}_1$ ,

$$v_2 \le J_\eta(\mu_2, \nu_2; f_1^*) < J_\eta(\mu_1, \nu_1; f_1^*) + C' = v_1 + C',$$

and similarly (interchanging roles), for any  $f_2^{\star} \in \mathcal{S}_2$ ,

$$v_1 \le J_{\eta}(\mu_1, \nu_1; f_2^{\star}) < J_{\eta}(\mu_2, \nu_2; f_2^{\star}) + C' = v_2 + C',$$
 getting  $|v_1 - v_2| < C' = C(\eta, \delta)\tau + 2diam(\mathcal{X})^2\delta$ .

Step 5: Choice of  $\tau, \eta, \delta$  given  $\varepsilon > 0$ . Similarly as in the proof of Theorem 7.13, we define

$$U_{\varepsilon}(\mathcal{S}_1) := \{ f \in \mathcal{F} \mid \|f - \mathcal{S}_1\|_{\infty} < \varepsilon \},\$$

where  $||f - S_1||_{\infty}$  denotes the  $L^{\infty}$ -distance between f and the compact set  $S_1$ . Define the "margin" around  $S_1$  by

$$m_{\varepsilon}^{(1)} := \inf_{f \in \mathcal{F} \setminus U_{\varepsilon}} J_{\eta}(\mu_1, \nu_1; f) - \min_{g \in \mathcal{F}} J_{\eta}(\mu_1, \nu_1; g).$$

Notice that  $m_{\varepsilon}^{(1)}>0$ : indeed, by definition  $m_{\varepsilon}^{(1)}\geq 0$ , and if  $m_{\varepsilon}^{(1)}=0$ , it would imply that there exists  $\widetilde{f}\in \mathcal{F}\setminus U_{\varepsilon}(\mathcal{S}_1)$  such that  $J_{\eta}(\mu_1,\nu_1;\widetilde{f})=v_1$ , i.e.,  $\widetilde{f}\in \mathcal{S}_1$  contradicting  $\|\widetilde{f}-\mathcal{S}_1\|_{\infty}\geq \varepsilon>0$  (where the existence of minimizer  $\widetilde{f}$  relies on the compactness of  $\mathcal{F}$  and the continuity of  $J_{\eta}$ ). which is positive by compactness of  $\mathcal{F}$  and continuity of  $J_{\eta}$ . Choose  $\delta\in(0,1)$  and  $\eta>0$  so that  $\eta t_{\delta,B}-L>0$  and the bad-event penalty obeys

$$2diam(\mathcal{X})^2 \delta \le m_{\varepsilon}^{(1)}/4. \tag{11}$$

Then choose

$$0 < \tau \le \frac{m_{\varepsilon}^{(1)}}{4 C(\eta, \delta)}. \tag{12}$$

As a consequence, we obtain

$$\left| \min_{f \in \mathcal{F}} J_{\eta}(\mu_1, \nu_1; f) - \min_{f \in \mathcal{F}} J_{\eta}(\mu_2, \nu_2; f) \right| < \frac{m_{\varepsilon}^{(1)}}{2}.$$

By the usual margin argument (similarly as in the proof of Theorem 7.13), this yields  $S_2 \subset U_{\varepsilon}(S_1)$ . See Figure 10 for a schematic visualization. In fact, if  $f_2^{\star} \in S_2$  but  $f_2^{\star} \in \mathcal{F} \setminus U_{\varepsilon}(S_1)$ , by definition of  $m_{\varepsilon}^{(1)}$ ,

$$v_1 + m_{\varepsilon}^{(1)} \le J_{\eta}(\mu_1, \nu_1; f_2^{\star}) < v_2 + \frac{m_{\varepsilon}^{(1)}}{2} < v_1 + m_{\varepsilon}^{(1)},$$

that is,  $m_{\varepsilon}^{(1)} < m_{\varepsilon}^{(1)}$ , which yields a contradiction. Changing the roles and defining the margin around  $S_2$ 

$$m_{\varepsilon}^{(2)} := \inf_{f \in \mathcal{F} \setminus U_{\varepsilon}} J_{\eta}(\mu_2, \nu_2; f) - \min_{g \in \mathcal{F}} J_{\eta}(\mu_2, \nu_2; g).$$

we have that under the choices:

1.  $\delta \in (0,1)$  and  $\eta > 0$  so that  $\binom{B}{2}(1-e^{-L/\eta}) < \delta \le m_\varepsilon^{(1)}/8diam(\mathcal{X})^2$ , and

2.  $\tau \leq \frac{m_{\varepsilon}^{(2)}}{4C(\eta,\delta)}$ , we get  $S_1 \subset U_{\varepsilon}(S_2)$ , where

$$U_{\varepsilon}(\mathcal{S}_2) := \{ f \in \mathcal{F} \mid \|f - \mathcal{S}_2\|_{\infty} < \varepsilon \}.$$

This part reads as the thesis of Theorem 7.13: for every  $f_1^{\star} \in \mathcal{S}_1$ , under this choice of parameters  $\eta, \delta, \tau$  depending on  $\varepsilon > 0$ , we have  $\|f_2^{\star} - f_1^{\star}\|_{\infty} < \varepsilon$  for some  $f_2^{\star} \in \mathcal{S}_2$ .

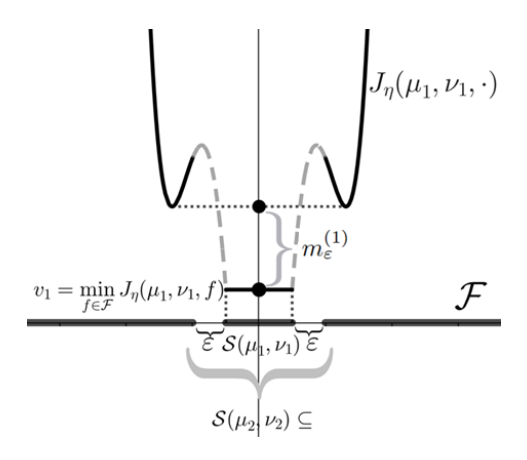


Figure 10. Sketch illustrating that  $S(\mu_2, \nu_2) \subset U_{\varepsilon}(S(\mu_1, \nu_1))$  if  $\tau$  is chosen appropriately depending on the gap  $m_{\varepsilon}^{(1)}$ .

**Note:** Notice that using these quantitative bounds, there exists a trade-off between  $\delta$  and  $\eta$ : Indeed, the condition  $\eta t_{\delta,B} > L$  (equivalently,  $\delta > {B \choose 2}(1-e^{-L/\eta})$ ) ensures that the slicers  $g_{\xi_{\eta}}$  are uniformly inverse-Lipschitz on a high-probability event. Larger values of  $\eta$  make this condition easier to satisfy (allowing smaller  $\delta$ ), while smaller  $\eta$  forces  $\delta$  to be larger. On the other hand, the final stability bound requires  $\delta$  to be sufficiently small in order to control the bad-event penalty.

Comment: For a fixed pair of source-target  $(\mu, \nu)$  measures,  $J_{\eta}$  is Lipschitz with respect to  $(\mathcal{F}, \|\cdot\|_{\infty})$  with high probability. Here we repeat some arguments from step 3 but, instead of fixing  $f \in \mathcal{F}$  and varying  $\mu_i, \nu_i \in \mathcal{P}(X)$  (i=1,2), we fix a pair of source-target measures  $\mu, \nu \mathcal{P}(\mathcal{X})$  and consider two different arbitrary slicers  $f_1, f_2 \in \mathcal{F}$ .

Let  $f_1, f_2 \in \mathcal{F}$ . Fix a realization of Z and set

$$g^{(i)}(x):=g^{f_i}_{\xi_n}(x)=f_i(x)+\eta\langle Z,x\rangle \qquad i=1,2.$$

Then for all  $x \in \mathcal{X}$ ,

$$|g^{(1)}(x) - g^{(2)}(x)| = |f_1(x) - f_2(x)| \le ||f_1 - f_2||_{\infty}.$$
  
Let  $u, v \in \mathcal{P}(\mathcal{X}).$ 

For i=1,2, let  $\alpha_{f_i}^{(Z)}:=(g^{(i)})_\#\mu$  and  $\beta_{f_i}^{(Z)}:=(g^{(i)})_\#\nu$ ; let  $\sigma_{f_i}^{(Z)}$  be the *unique* 1D optimal plan between  $\alpha_{f_i}^{(Z)},\beta_{f_i}^{(Z)}$ , with corresponding *unique* lifted coupling  $\gamma_{f_i}^{(Z)}\in\Gamma(\mu,\nu)$  such that  $(g^{(i)},g^{(i)})_\#\gamma_i^{(Z)}=\sigma_i^{(Z)}$ . By Lemma 7.5, for the pushforwards of  $\mu$  we obtain

$$W_2(\alpha_{f_1}^{(Z)}, \alpha_{f_2}^{(Z)}) \le ||f_1 - f_2||_{\infty},$$

and similarly for the pushforwards of  $\nu$ ,

$$W_2(\beta_{f_1}^{(Z)}, \beta_{f_2}^{(Z)}) \leq ||f_1 - f_2||_{\infty}.$$

Applying Lemma 7.6, we get

$$W_{2}(\sigma_{f_{1}}^{(Z)}, \sigma_{f_{2}}^{(Z)}) \leq \left(W_{2}^{2}(\alpha_{f_{1}}^{(Z)}, \alpha_{f_{2}}^{(Z)}) + W_{2}^{2}(\beta_{f_{1}}^{(Z)}, \beta_{f_{2}}^{(Z)})\right)^{1/2}$$
$$\leq \sqrt{2} \|f_{1} - f_{2}\|_{\infty}.$$

As a consequence of steps 1 and 2 and the above inequality,

$$\begin{aligned} \left| J_{\eta}(\mu, \nu; f_{1}) - J_{\eta}(\mu, \nu; f_{2}) \right| \\ &= \left| \mathbb{E}_{Z} \left[ \int c^{2} d\gamma_{f_{1}}^{(Z)} - \int c^{2} d\gamma_{f_{2}}^{(Z)} \right] \right| \\ &\leq \mathbb{E}_{Z} \left[ \left| \int c^{2} d\gamma_{f_{1}}^{(Z)} - \int c^{2} d\gamma_{f_{2}}^{(Z)} \right| \right] \\ &\leq 4 \operatorname{diam}(\mathcal{X}) \|f_{1} - f_{2}\|_{\infty} \mathbb{E}_{Z}[K_{Z} \mathbf{1}_{G}] + 2 \operatorname{diam}(\mathcal{X})^{2} \delta \\ &\leq \frac{4 \operatorname{diam}(\mathcal{X}) (1 - \delta)}{\eta t_{\delta, B} - L} \|f_{1} - f_{2}\|_{\infty} + 2 \operatorname{diam}(\mathcal{X})^{2} \delta. \end{aligned}$$

### 8. Statistical Properties of Minibatch Training

In this section, we consider the minibatch training of the slicer over finite discrete samples. In each minibatch, samples are reweighted to have uniform mass.

**Definition 8.1** (Minibatch STP loss as a two-sample U-statistic). Let  $X = \{x_i\}_{i=1}^N$  and  $Y = \{y_j\}_{j=1}^M$  be two sets of discrete samples, and write  $[n] := \{1, \ldots, n\}$ . Fix a batch size  $B \le \min(N, M)$ . Define the two-sample kernel for batches  $x_{i_1:i_B}$  and  $y_{j_1:j_B}$  with slicer  $f : \mathbb{R}^d \to \mathbb{R}$  as

$$h_B(f; x_{i_1:i_B}, y_{j_1:j_B}) := \frac{1}{B} \sum_{i=1}^B d(x_{(i)}^f, y_{(i)}^f)^p,$$

where  $x_{(i)}^f$ ,  $y_{(i)}^f \in \mathbb{R}^d$  denote the re-ordered  $x_{i_1:i_B}$  and  $y_{j_1:j_B}$ , paired by the lifted coupling from 1D optimal coupling, i.e.  $f(x_{(1)}^f) \leq \cdots \leq f(x_{(B)}^f)$  and  $f(y_{(1)}^f) \leq \cdots \leq f(y_{(B)}^f)$  for the slicer  $f: \mathbb{R}^d \to \mathbb{R}$ .

The minibatch STP loss (U-statistic of order B, B) for a slicer  $f : \mathbb{R}^d \to \mathbb{R}$  is defined as

$$J_{N,M,B}(f) := \frac{1}{\binom{N}{B}\binom{M}{B}} \sum_{S \in \binom{[N]}{B}} \sum_{T \in \binom{[M]}{B}} h_B(f; x_S, y_T),$$

where S is the set of B indices drawn from [N] without replacement and T is the set of B indices drawn from [M] without replacement.  $x_S = (x_i)_{i \in S}$  and  $y_T = (y_i)_{i \in T}$ .

The incomplete estimator draws K i.i.d. pairs  $\{(S_k, T_k)\}_{k=1}^K$  uniformly from  $\binom{[N]}{B} \times \binom{[M]}{B}$ , and averages:

$$\overline{J}_{B,K}(f) := \frac{1}{K} \sum_{k=1}^{K} h_B(f; x_{S_k}, y_{T_k}).$$

In the following context,  $(S,T) \sim \mathrm{Unif}\left(\binom{[N]}{B} \times \binom{[M]}{B}\right)$ . (i.e., uniform distribution over all size-B subsets.)

**Proposition 8.2** (Incomplete vs. complete deviation). Fix the datasets  $X = \{x_i\}_{i=1}^N, Y = \{y_j\}_{j=1}^M$ . Let  $R := \max_{i,j} d(x_i, y_j)^p$ . Then  $\mathbb{E}_{S,T}[h_B(f; x_S, y_T)] = J_{N,M,B}(f)$  and, for any  $\epsilon > 0$ ,

$$\Pr(\left|\overline{J}_{B,K}(f) - J_{N,M,B}(f)\right| \ge \epsilon) \le 2\exp\left(-\frac{2K\epsilon^2}{R^2}\right).$$

In particular,

$$\operatorname{Var}(\overline{J}_{B,K}(f)) \leq \frac{R^2}{4K},$$

$$\mathbb{E}[|\overline{J}_{B,K}(f) - J_{N,M,B}(f)|] \leq \frac{R}{2\sqrt{K}}.$$

Proof. By definition,

$$J_{N,M,B}(f) = \frac{1}{\binom{N}{B}\binom{M}{B}} \sum_{S \in \binom{[N]}{B}} \sum_{T \in \binom{[M]}{B}} h_B(f; x_S, y_T),$$

so taking expectation over a uniformly chosen (S, T) yields

$$\mathbb{E}_{S,T} h_B(f; x_S, y_T) = J_{N,M,B}(f).$$

Next, for each draw  $\{(S_k, T_k)\}_{k=1}^K$ ,

$$\overline{J}_{B,K}(f) = \frac{1}{K} \sum_{k=1}^{K} h_B(f; x_{S_k}, y_{T_k}).$$

Since each summand in  $h_B$  is of the form  $d(x_{(i)}^f, y_{(i)}^f)^p \in [0, R]$ , we have  $0 \le h_B(f; x_S, y_T) \le R$  for all S, T. Hence, the variables  $h_B(f; x_{S_k}, y_{T_k})$  are i.i.d. and lie in [0, R].

Applying Hoeffding's inequality to  $\overline{J}_{B,K}(f)$  gives, for any  $\epsilon > 0$ ,

$$\Pr(\left|\overline{J}_{B,K}(f) - \mathbb{E}\overline{J}_{B,K}(f)\right| \ge \epsilon) \le 2\exp\left(-\frac{2K\epsilon^2}{R^2}\right).$$

Using  $\mathbb{E}\overline{J}_{B,K}(f) = \mathbb{E}_{S,T} h_B(f; x_S, y_T) = J_{N,M,B}(f)$  yields the stated tail bound.

For the variance bound, by independence,

$$\operatorname{Var}(\overline{J}_{B,K}(f)) = \frac{1}{K} \operatorname{Var}(h_B(f; x_S, y_T)) \le \frac{1}{K} \cdot \frac{R^2}{4} = \frac{R^2}{4K},$$

where we used that a random variable supported on an interval of length R has variance at most  $R^2/4$ . Finally, by Cauchy–Schwarz,

$$\mathbb{E}\big[\big|\overline{J}_{B,K}(f) - J_{N,M,B}(f)\big|\big] \le \sqrt{\operatorname{Var}\big(\overline{J}_{B,K}(f)\big)} \le \frac{R}{2\sqrt{K}}.$$

**Lemma 8.3** (McDiarmid's Inequality for two i.i.d. samples). Let  $X,Y \subset \mathbb{R}^d$ ,  $\mu \in \mathcal{P}(X)$ ,  $\nu \in \mathcal{P}(Y)$ . Let  $F: X^N \times Y^M \to \mathbb{R}$  for  $N,M \geq 1$ . Assume for all  $1 \leq i \leq N, 1 \leq j \leq M$ , the change of F by substituting one coordinate is bounded, i.e. there exists  $a_i$  and  $b_j$  such that

$$|F(\ldots, x_i, \ldots; y) - F(\ldots, x'_i, \ldots; y)| \le a_i,$$
  

$$|F(x; \ldots, y_j, \ldots) - F(x; \ldots, y'_j, \ldots)| \le b_j.$$

where  $x \in X^N, y \in Y^M$  and  $x_i, x_i' \in X, y_j, y_j' \in Y$ . If  $x_1, \ldots, x_N \overset{i.i.d.}{\sim} \mu$  and  $y_1, \ldots, y_M \overset{i.i.d.}{\sim} \nu$  are all independent, then

$$\Pr(\left| F(x_{1:N}, y_{1:M}) - \mathbb{E}F(x_{1:N}, y_{1:M}) \right| \ge \epsilon)$$

$$\le 2 \exp\left( -\frac{2\epsilon^2}{\sum_{i=1}^{N} a_i^2 + \sum_{j=1}^{M} b_j^2} \right).$$

*Proof.* Let m:=N+M and define the independent sequence  $Z=\{z_l\}_{l=1}^m$  with  $z_1:=x_1,\ldots,z_N:=x_N,z_{N+1}:=y_1,\ldots,z_m:=y_M.$  With a slight abuse of notation, we write  $F(Z):=F(x_{1:N},y_{1:M})$  and the Doob martingale  $M_l:=\mathbb{E}[F(Z)\mid z_1,\ldots,z_l]$  for  $l=1,\ldots,m$  and  $M_0=\mathbb{E}(F(Z))$ , with increments  $\Delta_l:=M_l-M_{l-1}$  for  $1\leq l\leq m$ .

Fix l and the prefix  $(z_1,\ldots,z_{l-1})$ . Consider  $\varphi_l(z):=\mathbb{E}[F(z_1,\ldots,z_{l-1},z,z_{l+1},\ldots,z_m)|z_1,\ldots,z_{l-1}]$ . By the bounded-differences assumption on the lth coordinate,  $|\varphi_l(z)-\varphi_l(z')|\leq \alpha_l$  for  $z,z'\in X$  or  $z,z'\in Y$ , where

$$\alpha_l = \begin{cases} a_l, & l \le N, \\ b_{l-N}, & l > N. \end{cases}$$

Hence  $\Delta_l = \varphi_l(z_l) - \mathbb{E}[\varphi_l(z_l) \mid z_1, \dots, z_{l-1}]$  is centered and supported in an interval of length at most  $\alpha_l$ . By Hoeffding's lemma,

$$\mathbb{E}\left[e^{\lambda\Delta_l}\mid z_1,\ldots,z_{l-1}\right] \leq \exp\left(\frac{\lambda^2\alpha_l^2}{8}\right).$$

Iterating and using the tower property,

$$\mathbb{E} e^{\lambda(F - \mathbb{E}F)} = \mathbb{E} e^{\lambda \sum_{l=1}^{m} \Delta_l}$$

$$\leq \exp\left(\frac{\lambda^2}{8} \sum_{l=1}^{m} \alpha_l^2\right)$$

$$= \exp\left(\frac{\lambda^2}{8} \left(\sum_{i=1}^{N} a_i^2 + \sum_{i=1}^{M} b_j^2\right)\right).$$

By Chernoff's method,

$$\Pr(F - \mathbb{E}F \ge \epsilon) \le \exp\left(-\lambda \epsilon + \frac{\lambda^2}{8} \left(\sum_i a_i^2 + \sum_j b_j^2\right)\right).$$

Optimizing at  $\lambda^{\star} = \frac{4\epsilon}{\sum_{i} a_{i}^{2} + \sum_{j} b_{j}^{2}}$  gives

$$\Pr(F - \mathbb{E}F \ge \epsilon) \le \exp\left(-\frac{2\epsilon^2}{\sum_i a_i^2 + \sum_j b_j^2}\right).$$

Apply the same to  $-(F - \mathbb{E}F)$  and we can obtain

$$\Pr(\left|F - \mathbb{E}F\right| \ge \epsilon) \le 2 \exp\left(-\frac{2\epsilon^2}{\sum_{i=1}^N a_i^2 + \sum_{j=1}^M b_j^2}\right).$$

**Proposition 8.4** (Dataset  $\rightarrow$  population deviation, fixed f). Let  $x_{1:N} \stackrel{i.i.d.}{\sim} \mu$  and  $y_{1:M} \stackrel{i.i.d.}{\sim} \nu$ . Fix f and a batch size  $B \leq \min(N, M)$ . Assume  $d(x, y) \leq D$  on  $\mathcal X$  and set  $R := D^p$ . Define the population target  $J_B(f) := \mathbb{E} h_B(f; x_{i_1:i_B}, y_{j_1:j_B})$  with  $x_{i_1:i_B} \sim \mu^{\otimes B}$  and  $y_{j_1:j_B} \sim \nu^{\otimes B}$ . Then, for any  $\epsilon > 0$ ,

$$\Pr(|J_{N,M,B}(f) - J_B(f)| \ge \epsilon)$$

$$\le 2 \exp\left(-\frac{2\epsilon^2}{B^2 R^2 \left(\frac{1}{N} + \frac{1}{M}\right)}\right).$$

*Proof.*  $J_{N,M,B}(f)$  is a two-sample U-statistic with kernel  $h_B$ , hence  $\mathbb{E} J_{N,M,B}(f) = J_B(f)$ .

View  $J_{N,M,B}(f)$  as a function of the independent inputs  $(x_1,\ldots,x_N,y_1,\ldots,y_M)$ . Replacing a single  $x_i$  affects exactly the fraction  $\binom{N-1}{B-1}/\binom{N}{B}=B/N$  of the summands; since each summand lies in [0,R] we have a change of at most (B/N)R. Similarly, replacing a single  $y_j$  changes

the value by at most (B/M)R. McDiarmid's inequality with bounded differences  $a_i = (B/N)R$  for each  $x_i$  and  $b_j = (B/M)R$  for each  $y_j$  yields

$$\Pr\left(|J_{N,M,B}(f) - \mathbb{E}J_{N,M,B}(f)| \ge \epsilon\right)$$

$$\le 2\exp\left(-\frac{2\epsilon^2}{\sum_i a_i^2 + \sum_j b_j^2}\right)$$

$$= 2\exp\left(-\frac{2\epsilon^2}{B^2R^2\left(\frac{1}{N} + \frac{1}{M}\right)}\right),$$

and  $\mathbb{E}J_{N,M,B}(f) = J_B(f)$  finishes the proof.

**Lemma 8.5** (Subadditivity and scale control for moduli of continuity). Let  $I \subset \mathbb{R}$  be an interval and  $g: I \to \mathbb{R}$ . Define the modulus of continuity

$$\omega_g(t) := \sup_{\substack{x,y \in I \\ |x-y| \le t}} |g(x) - g(y)|, \quad t \ge 0.$$

Then  $\omega_a(t)$  has the following properties

- (i) (Monotonicity)  $\omega_q(0) = 0$  and  $\omega_q$  is nondecreasing.
- (ii) (Subadditivity) For all  $s, t \geq 0$ ,

$$\omega_q(s+t) \leq \omega_q(s) + \omega_q(t).$$

(iii) (Scale-specific linear bound) For any  $\eta > 0$  and all  $t \ge 0$ ,

$$\omega_g(t) \leq \left(\frac{t}{\eta} + 1\right) \omega_g(\eta).$$

Proof. (i) Trivial: the supremum over an empty displacement is 0; enlarging the admissible set in t cannot decrease the supremum.

(ii) Fix  $x,y\in I$  with  $|x-y|\leq s+t$ . Choose z on the segment [x,y] so that  $|x-z|\leq s$  and  $|z-y|\leq t$  (possible since I is an interval). Then

$$|g(x)-g(y)| \le |g(x)-g(z)|+|g(z)-g(y)| \le \omega_g(s)+\omega_g(t).$$

Taking the supremum over such x, y gives  $\omega_g(s+t) \le \omega_g(s) + \omega_g(t)$ .

(iii) Write  $t = m\eta + r$  with  $m = \lfloor t/\eta \rfloor \in \mathbb{N}$  and  $r \in [0, \eta)$ . By (ii),

$$\begin{split} \omega_g(t) \; &= \; \omega_g(m\eta + r) \; \leq \; m \, \omega_g(\eta) + \omega_g(r) \\ &\leq \; (m+1) \, \omega_g(\eta) \; = \; \left( \left\lceil \frac{t}{\eta} \right\rceil \right) \omega_g(\eta), \end{split}$$

and since  $\lceil t/\eta \rceil \leq t/\eta + 1,$  the second inequality follows.

**Corollary 8.6** (Scale-specific linearization in expectation). Let  $T \geq 0$  be any random variable with  $\mathbb{E}T < \infty$ . For any  $\eta > 0$ ,

$$\mathbb{E} \,\omega_g(T) \leq \omega_g(\eta) \left(\frac{\mathbb{E}T}{\eta} + 1\right).$$

**Proposition 8.7** (Minibatch  $\rightarrow$  full STP gap under bi-Lipschitz slicer). Let  $X = \{x_i\}_{i=1}^N$ ,  $Y = \{y_j\}_{j=1}^M$  and  $f: \mathbb{R}^d \rightarrow \mathbb{R}$ . Define  $\mu_N = \frac{1}{N} \sum_{i=1}^N \delta_{x_i}$ ,  $\nu_M = \frac{1}{M} \sum_{j=1}^M \delta_{y_j}$  and let  $\gamma = \{\gamma_{ij}\}$  be the lifted plan from the 1D optimal transport plan between  $f_{\#}\mu_N$  and  $f_{\#}\nu_M$ , with  $\gamma_{ij} \geq 0$ ,  $\sum_j \gamma_{ij} = 1/N$ ,  $\sum_i \gamma_{ij} = 1/M$ . Recall the STP $_p^p$  objective. For convenience we denote it as  $J_{N,M}$  in connection to the minibatch version:

$$J_{N,M}(f) := \sum_{i=1}^{N} \sum_{j=1}^{M} \gamma_{ij} d(x_i, y_j)^p.$$

Assume there exist constants  $c_X, c_Y > 0$  and  $L_X, L_Y \ge 0$  such that

$$|f(x) - f(x')| \ge c_X d(x, x')$$
 for all  $x, x' \in X$ ,
$$(13)$$

$$|f(y) - f(y')| \ge c_Y d(y, y')$$
 for all  $y, y' \in Y$ ,
$$(14)$$

$$|d(x,y)^p - d(x',y')^p| \le L_X d(x,x') + L_Y d(y,y')$$
(15)

for all 
$$x, x', y, y'$$
.

Write the projected oscillations

$$\mathcal{O}_X(f) := \max_{x \in X} f(x) - \min_{x \in X} f(x),$$
  
$$\mathcal{O}_Y(f) := \max_{y \in Y} f(y) - \min_{y \in Y} f(y).$$

Then, deterministically (for the fixed datasets X, Y),

$$\left| J_{N,M,B}(f) - J_{N,M}(f) \right| \le \frac{1}{B} \left( \frac{L_X}{c_X} \mathcal{O}_X(f) + \frac{L_Y}{c_Y} \mathcal{O}_Y(f) \right)$$
$$+ 2 \frac{L_X}{c_Y} \omega_X \left( \frac{1}{2} \sqrt{\frac{N-B}{NB}} \right) + 2 \frac{L_Y}{c_Y} \omega_Y \left( \frac{1}{2} \sqrt{\frac{M-B}{MB}} \right).$$

where  $\omega_X$ ,  $\omega_Y$  are the quantile moduli for the pushforward empirical measures  $f_{\#}\mu_N$  and  $f_{\#}\nu_M$  (nondecreasing, zero at 0, step-like in the discrete case).

*Proof.* Order the samples by the slicer:  $f(x_{(1)}^f) \leq \cdots \leq f(x_{(N)}^f)$  and  $f(y_{(1)}^f) \leq \cdots \leq f(y_{(M)}^f)$ . Define the stepwise-constant "quantile selectors"

$$X_f(u) := x_{(i)}^f \text{ for } u \in ((i-1)/N, i/N],$$
  
 $Y_f(u) := y_{(j)}^f \text{ for } u \in ((j-1)/M, j/M].$ 

Then the full objective admits the integral form

$$J_{N,M}(f) = \int_0^1 d(X_f(u), Y_f(u))^p du.$$
 (16)

Partition [0,1] into B equal sub-intervals  $I_k =$ ((k-1)/B, k/B], and assume  $u_k \in I_k, v_k \in I_k$  be the rank locations of the k-th order statistics of a size-Bsubset from X and Y respectively, i.e. the minibatch is constructed by picking one pair of points from each  $I_k$ . For any such subset pair (S, T),

$$h_B(f; x_S, y_T) = \frac{1}{B} \sum_{k=1}^B d(X_f(u_k), Y_f(v_k))^p.$$

Fix a block  $I_k = ((k-1)/B, k/B]$ . Define the bivariate

$$\mathscr{D}_{\times}(u,v) := d(X_f(u), Y_f(v))^p, \qquad (u,v) \in [0,1]^2,$$

and the diagonal (comonotone) integrand

$$\mathscr{D}(u) := \mathscr{D}_{\times}(u, u) = d(X_f(u), Y_f(u))^p.$$

Let the bin average be

$$\overline{\mathscr{D}}_k := B \int_{I_k} \mathscr{D}(u) du.$$

Then for  $u_k, v_k \in I_k$ ,

$$\begin{split} \left| \frac{1}{B} \, \mathscr{D}_{\times}(u_k, v_k) - \int_{I_k} \mathscr{D}(u) \, \mathrm{d}u \right| &= \frac{1}{B} \, \left| \mathscr{D}_{\times}(u_k, v_k) - \overline{\mathscr{D}}_k \right| \\ &\leq \frac{1}{B} \, \mathcal{O}_{I_k \times I_k}(\mathscr{D}_{\times}), \end{split}$$

where  $\mathcal{O}_{I_k \times I_k}(\mathscr{D}_{\times}) := \sup_{(u,v),(u',v') \in I_k \times I_k} |\mathscr{D}_{\times}(u,v) - \mathscr{D}_{\times}(u,v)|$  $\mathscr{D}_{\times}(u',v')|.$ 

Next, bound the bin oscillation via the Lipschitz and bi-Lipschitz assumptions: for any  $(u, v), (u', v') \in I_k \times I_k$ ,

$$\begin{split} &\left| \mathscr{D}_{\times}(u,v) - \mathscr{D}_{\times}(u',v') \right| \\ &= \left| d(X_f(u),Y_f(v))^p - d(X_f(u'),Y_f(v'))^p \right| \\ &\leq L_X d(X_f(u),X_f(u')) + L_Y d(Y_f(v),Y_f(v')) \\ &\leq \frac{L_X}{c_X} \left| f(X_f(u)) - f(X_f(u')) \right| \\ &+ \frac{L_Y}{c_Y} \left| f(Y_f(v)) - f(Y_f(v')) \right|. \end{split}$$

Taking supremum over  $I_k \times I_k$  yields

$$\mathcal{O}_{I_k \times I_k}(\mathscr{D}_\times) \, \leq \, \frac{L_X}{c_X} \, \mathcal{O}_{I_k} \big( f \circ X_f \big) + \frac{L_Y}{c_Y} \, \mathcal{O}_{I_k} \big( f \circ Y_f \big).$$

Summing over k = 1, ..., B and using monotonicity of  $f \circ X_f$  and  $f \circ Y_f$ ,

$$\begin{split} &\sum_{k=1}^B \mathcal{O}_{I_k} \big(f \circ X_f\big) = \mathcal{O}_{[0,1]} \big(f \circ X_f\big) = \mathcal{O}_X(f), \\ &\sum_{k=1}^B \mathcal{O}_{I_k} \big(f \circ Y_f\big) = \mathcal{O}_{[0,1]} \big(f \circ Y_f\big) = \mathcal{O}_Y(f). \end{split}$$

Therefore,

$$\left| \frac{1}{B} \sum_{k=1}^{B} \mathscr{D}_{\times}(u_{k}, v_{k}) - \int_{0}^{1} \mathscr{D}(u) \, \mathrm{d}u \right|$$

$$\leq \frac{1}{B} \left( \frac{L_{X}}{c_{X}} \, \mathcal{O}_{X}(f) + \frac{L_{Y}}{c_{Y}} \, \mathcal{O}_{Y}(f) \right),$$

and since  $\int_0^1 \mathscr{D}(u) du = J_{N,M}(f)$  and  $h_B(f; x_S, y_T) =$  $\frac{1}{B}\sum_{k=1}^B \mathscr{D}_{\times}(u_k,v_k)$ , the minibatch–full gap bound follows.

Now, if the samples are not stratified, we introduce another bound for the mismatch. Let  $S \subset [N]$ ,  $T \subset [M]$ be drawn uniformly without replacement (independently), with |S| = |T| = B, and let  $X_{f,S}, Y_{f,T}$  be the corresponding batch selectors. Then

$$h_B(f; x_S, y_T) = \frac{1}{B} \sum_{k=1}^{B} d(X_{f,S}(u_k), Y_{f,T}(v_k))^p,$$
$$u_k, v_k \in I_k.$$

Add and subtract the full selectors at the same  $(u_k, v_k)$  and use the triangle inequality:

$$\left| h_{B}(f; x_{S}, y_{T}) - J_{N,M}(f) \right|$$

$$\leq \left| \frac{1}{B} \sum_{k=1}^{B} d(X_{f}(u_{k}), Y_{f}(v_{k}))^{p} - \int_{0}^{1} d(X_{f}(u), Y_{f}(u))^{p} du \right|$$

$$+ \underbrace{\frac{1}{B} \sum_{k=1}^{B} \left| d(X_{f,S}(u_{k}), Y_{f,T}(v_{k}))^{p} - d(X_{f}(u_{k}), Y_{f}(v_{k}))^{p} \right|}_{A}.$$

The first term is already bounded by  $\frac{1}{B} \left( \frac{L_X}{c_X} \mathcal{O}_X(f) \right) +$  $\frac{L_Y}{c_Y}\mathcal{O}_Y(f)$ ). For the mismatch term,

$$\begin{aligned} &\left| d\left(X_{f,S}(u_k), Y_{f,T}(v_k)\right)^p - d\left(X_f(u_k), Y_f(v_k)\right)^p \right| \\ &\leq L_X d\left(X_{f,S}(u_k), X_f(u_k)\right) + L_Y d\left(Y_{f,T}(v_k), Y_f(v_k)\right) \\ &\leq \frac{L_X}{c_X} \Delta_X(u_k) + \frac{L_Y}{c_Y} \Delta_Y(v_k), \end{aligned}$$

where  $\Delta_X(u) := |f(X_{f,S}(u)) - f(X_f(u))|$  and similarly for  $\Delta_Y$ . Let  $Q_X(u), Q_Y(u)$  be the empirical quantile of  $f_{\#}\mu_X$ , and  $Q_{X,S}(u), Q_{Y,T}(u)$  be the quantile of the subsampled distributions. Then  $f \circ X_f(u) = Q_X(u)$ ,  $f \circ X_{f,S}(u) = Q_{X,S}(u)$  and  $\Delta_X(u) = |Q_X(u) - Q_{X,S}(u)|$ (and similarly for Y). Define the quantile modulus

$$\begin{split} \omega_X(\eta) &:= \sup_{\substack{u,v \in [0,1] \\ |u-v| \le \eta}} \Big| Q_X(u) - Q_X(v) \Big| \\ \omega_Y(\eta) &:= \sup_{\substack{u,v \in [0,1] \\ |u-v| \le \eta}} \Big| Q_Y(u) - Q_Y(v) \Big| \end{split}$$

For each  $k \in [B]$ , let  $\alpha_k$  (resp.  $\beta_k$ ) be the full-data index of the k-th order in the subsample from X (resp. Y), and define the actual full-data levels

$$U_k := \frac{\alpha_k}{N}, \qquad V_k := \frac{\beta_k}{M}.$$

Fix deterministic references  $u_k, v_k \in I_k = ((k-1)/B, k/B]$  (e.g.  $u_k = v_k = k/B$ ). Since  $f \circ X_{f,S}(u_k) = Q_X(U_k)$ , for each k,

$$|Q_{X,S}(u_k) - Q_X(u_k)| = |Q_X(U_k) - Q_X(u_k)|$$
  
$$\leq \omega_X(|U_k - u_k|),$$

and analogously  $\left|Q_{Y,T}(v_k) - Q_Y(v_k)\right| \leq \omega_Y(|V_k - v_k|)$ . Then

$$\left| d(X_{f,S}(u_k), Y_{f,T}(v_k))^p - d(X_f(u_k), Y_f(v_k))^p \right|$$

$$\leq \frac{L_X}{c_X} \omega_X (|U_k - u_k|) + \frac{L_Y}{c_Y} \omega_Y (|V_k - v_k|).$$

Averaging over  $k=1,\ldots,B$  and over all subsets (S,T) (i.e. taking expectation w.r.t. the uniform law on size-B subsets), we obtain the bound

$$\begin{aligned} & \left| J_{N,M,B}(f) - J_{N,M}(f) \right| \\ &= \left| \mathbb{E}_{S,T} h_B(f; x_S, y_T) - J_{N,M}(f) \right| \\ &\leq \mathbb{E}_{S,T} \left| h_B(f; x_S, y_T) - J_{N,M}(f) \right| \\ &\leq \frac{1}{B} \left( \frac{L_X}{c_X} \mathcal{O}_X(f) + \frac{L_Y}{c_Y} \mathcal{O}_Y(f) \right) \\ &+ \frac{1}{B} \sum_{k=1}^{B} \left( \frac{L_X}{c_X} \mathbb{E} \, \omega_X \left( |U_k - u_k| \right) + \frac{L_Y}{c_Y} \, \mathbb{E} \, \omega_Y \left( |V_k - v_k| \right) \right). \end{aligned}$$

For  $\mathbb{E}\omega_X(|U_k-u_k|)$  and  $\sigma=\frac{1}{2}\sqrt{\frac{N-B}{NB}}$  we have by Corollary 8.6,

$$\mathbb{E}\omega_X(|U_k - u_k|) \le \left(\frac{\mathbb{E}|U_k - u_k|}{\frac{1}{2}\sqrt{\frac{N-B}{NB}}} + 1\right)\omega_X\left(\frac{1}{2}\sqrt{\frac{N-B}{NB}}\right)$$
$$\le 2\omega_X\left(\frac{1}{2}\sqrt{\frac{N-B}{NB}}\right)$$

where the second inequality comes from the fact that sampling B points without replacement from N points gives

$$Var(U_k) \le \frac{N-B}{4BN}$$

and consequently

$$\mathbb{E}|U_k - u_k| \le \frac{1}{2} \sqrt{\frac{N - B}{NB}}.$$

Similarly,  $\mathbb{E}\omega_Y(|V_k-v_k|) \leq 2\omega_Y(\frac{1}{2}\sqrt{\frac{M-B}{MB}})$ . Therefore, we get the final bound

$$\begin{aligned} & \left| J_{N,M,B}(f) - J_{N,M}(f) \right| \\ & \leq \frac{1}{B} \left( \frac{L_X}{c_X} \, \mathcal{O}_X(f) + \frac{L_Y}{c_Y} \, \mathcal{O}_Y(f) \right) \\ & + 2 \frac{L_X}{c_X} \omega_X \big( \frac{1}{2} \sqrt{\frac{N-B}{NB}} \big) + 2 \frac{L_Y}{c_Y} \omega_Y \big( \frac{1}{2} \sqrt{\frac{M-B}{MB}} \big). \end{aligned}$$

**Corollary 8.8** (Global density lower bounds  $\Rightarrow$  linear moduli). Assume the pushforwards  $f_{\#}\mu_{N}$  and  $f_{\#}\nu_{M}$  admit densities  $p_{X}, p_{Y}$  on  $\mathbb{R}$  with  $p_{X}(z) \geq m_{X} > 0$  and  $p_{Y}(z) \geq m_{Y} > 0$  for all  $z \in \mathbb{R}$ . Then, for all  $t \in [0,1]$ ,

$$\omega_X(t) \le \frac{t}{m_X}, \qquad \omega_Y(t) \le \frac{t}{m_Y}.$$

Consequently,

$$\begin{aligned} & \left| J_{N,M,B}(f) - J_{N,M}(f) \right| \\ & \leq \frac{1}{B} \left( \frac{L_X}{c_X} \, \mathcal{O}_X(f) + \frac{L_Y}{c_Y} \, \mathcal{O}_Y(f) \right) \\ & + \frac{L_X}{c_X m_X} \sqrt{\frac{N-B}{NB}} + \frac{L_Y}{c_Y m_Y} \sqrt{\frac{M-B}{MB}}. \end{aligned}$$

**Remark 8.9** (Injective on finite  $\Rightarrow$  bi-Lipschitz on the samples). On a finite metric set (X,d), any injective  $f:X \to \mathbb{R}$  is bi-Lipschitz on X: define

$$c_X := \min_{\substack{x \neq x' \\ x, x' \in X}} \frac{|f(x) - f(x')|}{d(x, x')} > 0,$$

$$C_X := \max_{\substack{x \neq x' \\ x, x' \in X}} \frac{|f(x) - f(x')|}{d(x, x')} < \infty,$$

and analogously  $(c_Y, C_Y)$  on Y. Then  $c_X d(x, x') \le |f(x) - f(x')| \le C_X d(x, x')$  for all  $x, x' \in X$  (and the analogous inequality on Y). Therefore Assumption equation 13-equation 14 holds automatically for some  $c_X, c_Y > 0$ , and Proposition 8.7 applies.

#### 9. Experiment Details

In this section, we provide comprehensive experimental settings and implementation specifics to ensure full clarity and reproducibility.

#### 9.1. Transferability under Gradual Drift

#### 9.1.1. Model Configuration

We employ a Set-Transformer [27] architecture to process unordered point sets. The input consists of two-dimensional vectors (x, y), and the model outputs a scalar prediction for

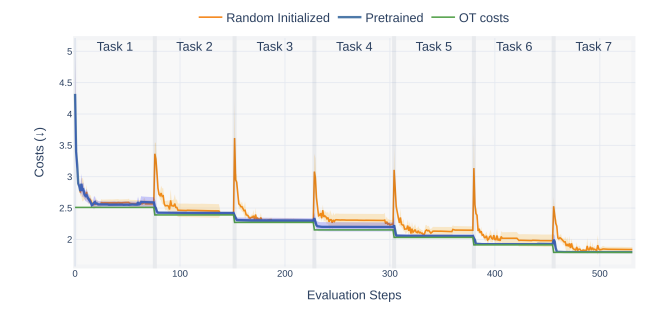


Figure 11. We plot the transport costs (over 5 runs) evaluated throughout the entire task sequence for two initialization strategies: randomly initialized slicer (orange), pretrained slicer (blue), and the exact OT costs (green) as a lower bound. The pretrained model exhibits fast convergence at each new task and maintains stable performance, whereas random initialization produces pronounced spikes at task boundaries before stabilizing.

each element. The encoder is composed of two stacked Induced Set Attention Blocks (ISAB), each with hidden dimension 64, 4 attention heads, and 16 learned inducing points, along with layer normalization. The ISAB modules implement a two-stage attention mechanism in which a fixed set of inducing vectors first attends to the input set and the input subsequently attends back to these induced features, providing an efficient and scalable approximation of full self-attention. The decoder consists of two Set Attention Blocks (SAB) with the same hidden dimension and number of heads, enabling global context propagation across all elements in the encoded representation. Finally, a linear mapping layer projects the decoder output to a one-dimensional scalar. This design leverages the Set-Transformer's inherent permutation equivariance and expressive attention-based aggregation, making it well-suited for learning functions over sets. The configurations are summarized in Table 2

Configuration Parameter	Value
Input dimension	2
Output dimension	1
Hidden dimension	64
Number of inducing points (ISAB)	16
Number of attention heads	4
Encoder structure	$ISAB \to ISAB$
Decoder structure	$SAB \to SAB$
Output layer	Linear $(64 \rightarrow 1)$

Table 2. Summary of the SetTransformer configuration used 4.1.

#### 9.1.2. Full Training Dynamics

Figure 11 shows the full evaluation trajectories for all seven tasks.

# 9.2. Amortized Min-STP for Point Cloud Alignment

#### **9.2.1.** Dataset

We used the ModelNet10 dataset [47], a curated subset of the Princeton ModelNet collection containing 10 object categories and 5000 CAD models, with 4078 shapes for training and 922 for testing. Following standard practice, we applied the NormalizeScale transform to center each shape and scale it to the unit sphere, ensuring consistent global geometry across the dataset. We then sampled 1024 points uniformly from the mesh surface using the SamplePoints (1024) transform, yielding point clouds  $X \in \mathbb{R}^{1024 \times 3}$  used to train the PointNet autoencoder. These normalized and uniformly sampled point clouds form the input for computing the context vectors used in our Model-Net10 alignment experiments.

Table 3. Statistics of the ModelNet10 dataset. Each object category contains CAD meshes converted to point clouds. Following standard practice, we sample 1024 points per shape using uniform surface sampling.

Category	# Train	# Test	Total
Bathtub	106	50	156
Bed	515	100	615
Chair	889	100	989
Desk	200	86	286
Dresser	200	86	286
Monitor	465	100	565
Night Stand	287	100	387
Sofa	680	100	780
Table	392	100	492
Toilet	344	100	444
Total	4,078	922	5,000

#### 9.2.2. Context Vectors

To obtain a compact representation of each 3D shape in ModelNet10, we pretrain a PointNet-style autoencoder on point clouds  $X \in \mathbb{R}^{N \times 3}$ . The encoder  $\phi$  applies a sequence of shared 1D convolutions and batch-normalization layers followed by global max pooling, producing a latent code  $c_X = \phi(X) \in \mathbb{R}^{512}$ . The decoder  $\psi$  maps  $c_X$  back to a reconstructed point set  $\hat{X} \in \mathbb{R}^{N \times 3}$ . We train the autoencoder end-to-end using the symmetric Chamfer distance between X and  $\hat{X}$  as the reconstruction loss, which encourages the latent code to capture the global geometry and coarse part structure of each object while remaining invariant to point permutations. After training, we discard the decoder and keep the encoder  $\phi$ . For every point cloud X used in our ModelNet10 alignment experiments, we compute its latent embedding  $c_X$  and use this vector as a *context vector* to condition the alignment model, allowing the learned transport

plans to adapt to the specific shape instance while sharing parameters across the dataset.

Table 4. Training hyperparameters used for the PointNet-style autoencoder

Hyperparameter	Value
Latent dimension $d_z$	512
Batch size	8 (ModelNet10)
Optimizer	Adam
Learning rate	$5 \times 10^{-4}$
Training epochs	1000
Point sampling	SamplePoints(1024)

## 10. Algorithms

In this section we present the key algorithms used in our method, including the mini-batch training procedure and the soft permutation operator. The mini-batch training procedure is detailed in Algorithm 1, with its workflow illustrated in Figure 3. For soft permutations, we borrowed the official implementation  $^1$  of LapSum [42]. However, the code was only for Soft Top-k Scores (see Algorithm 1 in [42]), here we show how we are constructing a Soft Permutation Matrix from Soft Top-k Scores. Given a score vector  $r \in \mathbb{R}^n$ , we generate a soft permutation matrix by repeatedly applying the soft top-k operator and then differencing the resulting cumulative masks. The procedure is:

1. Compute soft top-k masks for all k. For each  $k \in \{1, \ldots, n-1\}$ , apply the differentiable soft top-k operator to a copy of r:

$$softk_k = SoftTopK(r, k, \alpha),$$

producing a matrix softk  $\in \mathbb{R}^{(n-1)\times n}$  where each row is a softened indicator of the top-k elements.

Pad with boundary rows. Add a row of zeros at the top and a row of ones at the bottom:

$$R = egin{bmatrix} \mathbf{0}^{ op} \ ext{softk} \ \mathbf{1}^{ op} \end{bmatrix} \in \mathbb{R}^{(n+1) imes n}.$$

3. Difference consecutive rows to obtain a soft permutation. The soft permutation matrix is obtained by discrete differentiation:

$$P_{\ell i} = R_{\ell,i} - R_{\ell-1,i}, \qquad \ell = 1, \dots, n.$$

Each row of P corresponds to the (soft) probability that element i occupies rank  $\ell$  in the sorted order of r.

```
Algorithm 1: Mini-batch training with slicer f_{\theta}:
\mathbb{R}^{\bar{d}} \! \to \! \mathbb{R}
   Input: Datasets X = \{x_i\}_{i=1}^N, Y = \{y_j\}_{j=1}^M; batch
                      size B; mini-batches per epoch k; epochs E;
                      \alpha in LapSum; learning rate \eta
   Output: Optimal parameters \theta
   Precompute C_{ij} \leftarrow c(x_i, y_j).;
   Set a \leftarrow \frac{1}{N} \mathbf{1}_N, b \leftarrow \frac{1}{M} \mathbf{1}_M.;
   for e \leftarrow 1 to E do
             Set the batch gradient G \leftarrow 0.;
             for i \leftarrow 1 to k do
                      Draw random permutations \sigma of [N] and \tau
                        of [M].;
                      Select first B indices I \leftarrow \sigma[1:B],
                        J \leftarrow \tau[1:B].;
                      Set the pair of batches X_B \leftarrow X[I],
                        Y_B \leftarrow Y[J].;
                      u_x \leftarrow f_{\theta}(X_B), u_y \leftarrow f_{\theta}(Y_B).;
                \begin{array}{l} u_x \leftarrow J_{\theta}(\Lambda_B), u_y \leftarrow J_{\theta}(I_B).; \\ \tilde{P}_x \leftarrow \operatorname{LapSum}(u_x; \alpha) \ (\ref{alpha}), \\ P_y \leftarrow \operatorname{HardSort}(u_y), \gamma_1 \leftarrow \tilde{P}_x^{\top} P_y.; \\ P_x \leftarrow \operatorname{HardSort}(u_x), \\ \tilde{P}_y \leftarrow \operatorname{LapSum}(u_y; \alpha), \gamma_2 \leftarrow P_x^{\top} \tilde{P}_y.; \\ \tilde{\gamma}_B \leftarrow \frac{1}{2}(\gamma_1 + \gamma_2); \\ \mathcal{L}_i \leftarrow \frac{1}{B} \langle \tilde{\gamma}_B, C[I, J] \rangle.; \\ G \leftarrow G + \nabla_{\theta} \mathcal{L}_i.; \end{array}
             \theta \leftarrow \theta - \eta \cdot \frac{1}{\iota} G.;
   return \theta
```

<sup>1</sup>https://github.com/gmum/LapSum

# **Additional Experiments on Amortized Min-STP**

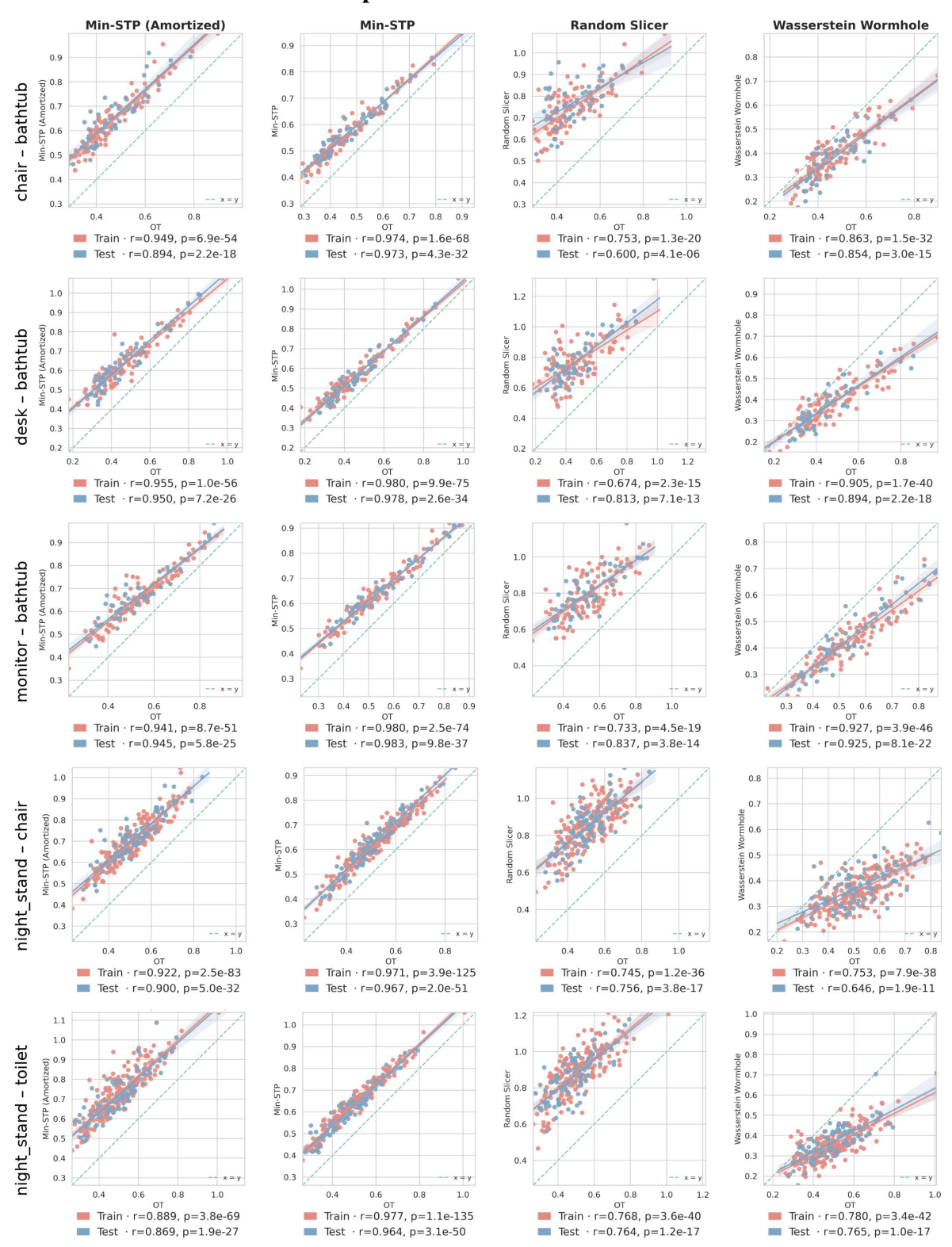


Figure 12. Additional experiments on amortized min-STP.